denaturation at 95°C for 15 s, followed by 40 cycles at 94°C for 1 s, 58°C for 10 s and 72°C for 15 s, followed by melting curve analysis. For analysis, quantitative amounts of ghrelin gene expression were standardized against the house-keeping gene b-actin, as previously described [23]. Quantitative data analysis was made possible by the use of ghrelin RNA from serially diluted gastric cDNA. A total of 10 ml of the reaction mixture were subsequently electrophoresed on a 1.6% agarose gel and visualized by ethidium bromide, using a 1 kb DNA ladder (GIBCO BRL) in order to estimate the band sizes. As a negative control for all the reactions, distilled water was used in place of cDNA. The RNA levels were expressed as a ratio, using "delta–delta method", for comparing relative expression results between treatments in real-time PCR. The primers used were Ghrelin: sense 59-TGA GCC CTG AAC ACC AGA GAG-39, antisense 59-AAA GCC AGA TGA GCG CTT CTA-39. The expected size for ghrelin is 327 bp; b actin: sense 59-AAG AGA GGC ATC CTC ACC CT-39, antisense 59-TAC ATG GCT GGG GTG TTG AA-39. The expected size for actin is 216 bp.

Statistical Analysis

Numerical values were expressed as mean ± standard deviation (SD) unless otherwise indicated. Differences in parameters between high and low groups were tested by Mann–Whitney's *U* test. The correlations among GPC score, BMI, and updated Sydney score with serum ghrelin levels were evaluated by Pearson's correlation coefficient test. A *P* value of <0.05 was considered statistically significant. StatView version 5.0 (SAS Institute, Inc, Cary, NC, USA) was used for statistical analysis.

Results

Distribution of Ghrelin Producing Cells and Its Scoring

The GPC in the stomach were small and round or spindle-shaped. GPC were abundant from the neck to the bottom in the fundic glands, but not observed in the foveolar epithelial cells, pyloric glands or intestinal metaplasia cells (Fig. 1). Half stomach, of either anterior or posterior wall, was prepared as 8-mm steps and 4-cm lengths of gastric sections on a slide glass, which were classified by the average number of GPC in the microscopic field as extra rich area (>40), rich area (20–40), middle area (1–20), or poor area (<1). Using this classification and proportion of each area, GPC score was calculated as representative of the sum total number of GPC for each patient. Mapping of GPC and GPC score

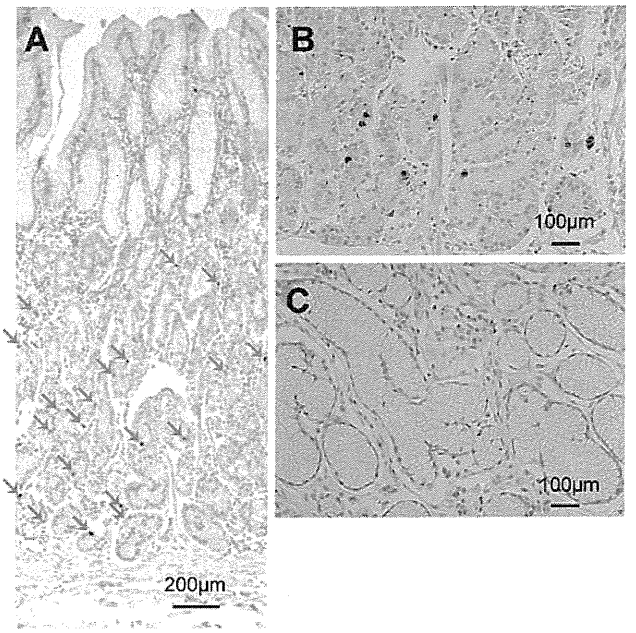

Fig. 1 Immunochemistry of ghrelin producing cells. Ghrelin producing cells (GPC) were stained by immunohistochemistry using anti ghrelin antibody. **a** Gastric mucosa in great curvature and corpus lesion showed GPC were not observed in the foveolar epithelial cells, but were abundant in the fundic glands (*arrows*) (×40). **b** Under higher magnification, GPC was recognized as small round or spindle cells with *brownish* stain in the cytoplasm (×400). **c** There were no GPC cells in the pyloric glands in the antrum (×400)

of 12 patients are shown in Fig. 2. GPC scores have shown approximately nine-fold differences among 12 patients ranging from 568 to 4511 (median 1472), and separated six patients into the high score group (median 2969; range 1791–4511) and six patients into the low score group (median 793; range 568–1153). It was a general trend that in the fundic gland area, GPC were more frequent in the greater curvature of the upper body and fornix and less frequent in the lesser curvature and anal and oral side. In the high score group, extra rich and rich areas tended to be dominant in the fundic gland area, while middle and poor areas were dominant in the low score group. Notably, some of the low score group (cases 7, 9, and 10), extra rich and/or rich area are still focally remaining.

Early gastric cancers which were small (size average 21 mm) and limited in the anterior or posterior wall were selected for this study. Gastric cancers were located in the anterior wall in two cases and posterior wall in ten cases, although the mapping image was inverted in the former in Fig. 2. None of cancer cells were positive for ghrelin immunohistochemistry. Symmetric distribution of GPC in the non-cancerous lesion was confirmed by comparing the number of GPC in the representative section located in the anterior and posterior walls of the upper body lesion (data not shown).

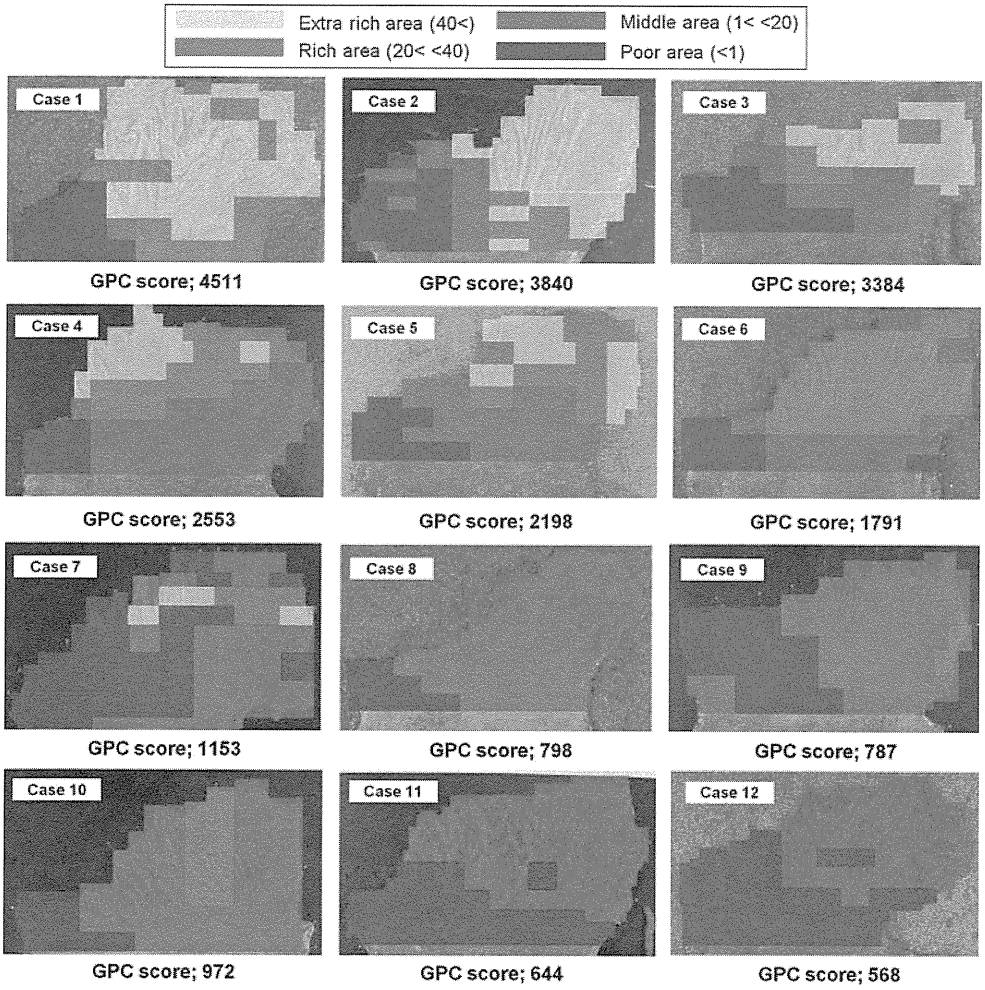

Fig. 2 Mapping of ghrelin producing cells (GPC) and GPC score of 12 patients. Half stomachs of 12 patients undergoing total gastrectomy due to early gastric cancers were subjected for GPC mapping. The number of GPC in each slide was classified as extra rich area (>40), rich area (20–40), middle area (1–20), or poor area (<1). Using this classification and proportion of each area, GPC score was calculated as representative of the sum total number of GPC for each patient. For cases 7 and 12, posterior half wall of the stomach was used for mapping and the image was inverted in this figure

GPC Score and Serum Ghrelin Levels

The average of serum total ghrelin levels was 65.7 ± 57.2 fmol/ml with large difference among patients ranging from 16.4 fmol/ml to 212.6 fmol/ml. There was a very strong and significant correlation among serum ghrelin levels and GPC score ($r = 0.75$, $P = 0.0047$, Fig. 3a). With respect to body weight, there was no correlation between BMI and GPC score ($r = 0.32$, $P = 0.31$, Fig. 3b). The inverse correlation between BMI and serum ghrelin, which was suggested in many previous studies, was not significant in this study ($r = -0.17$, $P = 0.60$, Fig. 3c). However, it is notable that in the GPC high score group, there was a trend that BMI showed negative correlation with serum ghrelin levels, while serum ghrelin levels were constantly low regardless of BMI in the low GPC score group (Fig. 3c). When focusing on two obese patients, serum ghrelin levels were relatively low despite high GPC score (arrows in Fig. 3a, b, c).

Chronic Gastritis and Ghrelin Feature

The degree of chronic gastritis was evaluated by updated Sydney System using H&E stained sections. As characteristic of early gastric cancer in Japan, ten of 12 patients showed moderate to severe chronic gastritis (Sydney score 5–10) and only two patients did not show significant gastritis less than 2 by updated Sydney score. In general, GPC was observed where fundic gland was preserved. However, we sometimes encountered absence of GPC in the fundic gland, where intestinal metaplasia and/or lymphocyte infiltration was prominent and thickness of fundic gland was declined.

There was significant inverse correlation of updated Sydney score with both GPC score and serum ghrelin, although the relationship was stronger with the former ($r = -0.84$, $P < 0.001$ and $r = -0.67$, $P = 0.016$, Fig. 4a, b). Besides updated Sydney score, various factors associated with chronic gastritis, including age, *H. pylori*

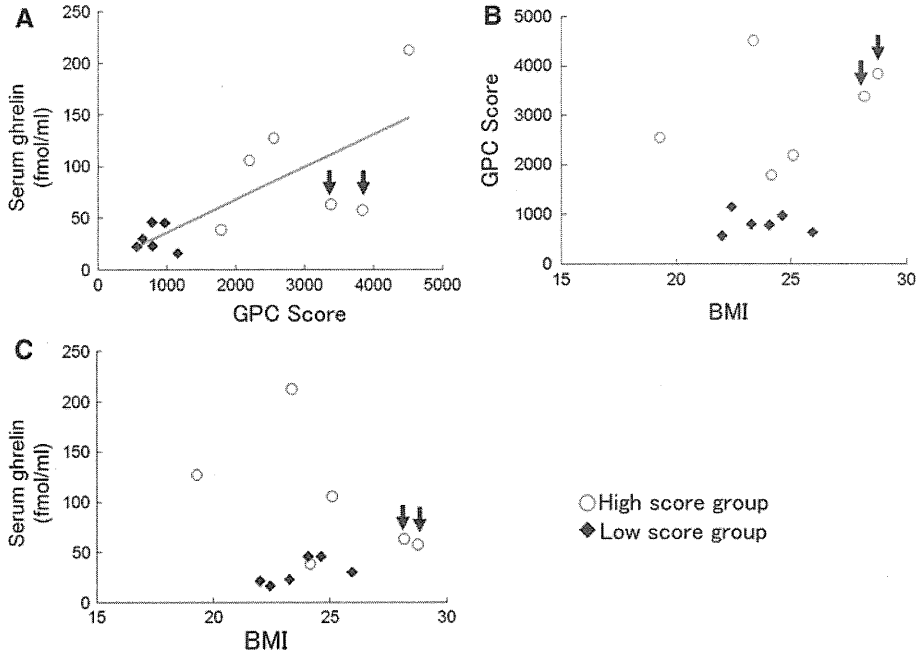

Fig. 3 The correlations among ghrelin producing cells (GPC) score, BMI, and serum ghrelin. Each two parameters among GPC score, BMI and serum total (acyl + des-acyl) ghrelin was plotted for 12 patients, who were classified as high (*open circle*) and low (*closed square*) GPC score. There was a significant correlation between serum ghrelin and GPC score ($r = 0.75$, $P = 0.0047$) (**a**), but BMI did not correlate with either GPC score ($r = 0.32$, $P = 0.31$) (**b**) or serum ghrelin ($r = -0.17$, $P = 0.60$) (**c**). Two patients with BMI greater than 28 were indicated by the *arrow*. They showed low serum ghrelin in spite of high GPC score

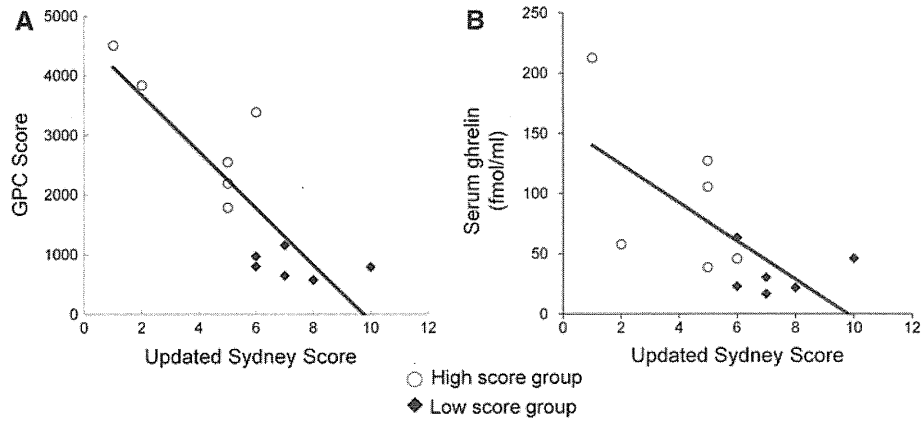

Fig. 4 The relationship between chronic gastritis and ghrelin profile. The degree of chronic gastritis was evaluated by updated Sydney score system, which was correlated with GPC score (**a**) and serum ghrelin (**b**). Patients were classified as high (*open circle*) and low (*closed square*) GPC score. Significant correlation was observed in both Fig. 5a ($r = -0.84$, $P < 0.001$) and 5b, ($r = -0.67$, $P = 0.016$)

infection, pepsinogen test and gastrin, were investigated for relationship with GPC score in Table 1. Age was not different between the two groups and females were more frequent in the high GPC group. Presence of *H. pylori* and pepsinogen positive test was more frequent and gastrin was higher in the GPC low group than in the GPC high group. With respect to histology of gastric cancer, intestinal type was more frequent in the GPC low group than in the GPC high group. However, these differences were not statistically significant due to a limited number of patients. When serum ghrelin was used for comparison instead of GPC score, serum ghrelin tended to be higher in females than in males (82.8 ± 39 vs. 60.0 ± 63, $P = 0.12$), in the *H. pylori* negative than in positive (106 ± 82 vs. 48.4 ± 28, $P = 0.27$) and in diffuse type than in intestinal type (101 ± 70 vs. 40.2 ± 31, respectively, $P = 0.019$). With respect to atrophic changes of gastric mucosa assessed by endoscopy, there were not significant associations between macroscopic mucosal change and GPC score.

Quantitative mRNA Assessment of Ghrelin Expression and the Number of Ghrelin Positive Cells

The quantitative mRNA of ghrelin expression was assessed from the biopsy samples by endoscopy before gastrectomy at each anatomical site of the stomach (Fig. 5a). The density of ghrelin-positive cells in gastric mucosa varied according to the anatomical site (Fig. 5b). The median number of ghrelin-positive cells at each anatomical section of mucosa was 74.5 in the fornix, 52 in the upper, 36 in the middle, and 23 in the lower stomach. There was an apparent correlation between ghrelin mRNA expression in gastric mucosa samples and ghrelin producing cell counts in immunohistochemistry ($R^2 = 0.87$, $P < 0.001$).

Table 1 Baseline characteristics

Parameter	Total	GPC score high group	GPC score low group	*P*
Age, median (year)	64.5 (45–83)	66.0 (54–74)	62.0 (45–83)	0.47[a]
Gender (male/female)	9/3	3/3	6/0	0.091[b]
BMI, median (kg/m^2)	24.1 (19.3–28.8)	24.6 (19.3–28.8)	23.7 (22.0–25.9)	0.50[a]
H. pylori infection (positive/negative)	8/4	3/3	5/1	0.27[b]
Pepsinogen test (positive/negative)	5/7	1/5	4/2	0.12[b]
Atrophic change (C-type/O-type)	5/7	2/4	3/3	0.56[b]
Gastric cancer differentiation (undiff/diff)	5/7	4/2	1/5	0.12[b]
Gastrin; median (pg/mL)	204 (95–630)	135 (95–240)	210 (100–630)	0.26[a]

[a] Mann–Whitney's *U* test

[b] Fisher's exact probability test

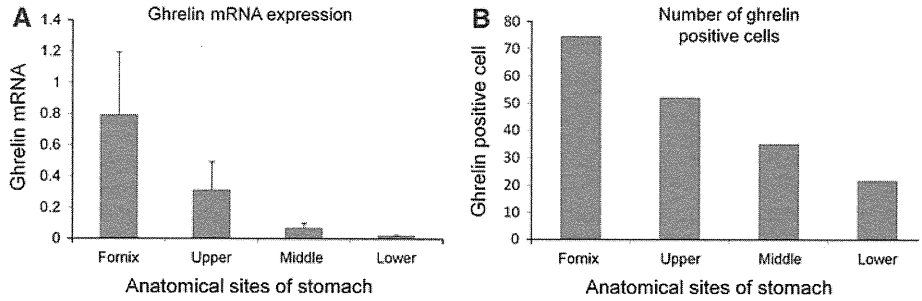

Fig. 5 Quantitative mRNA assessment of ghrelin expression and the number of ghrelin positive cells at each anatomical site of the stomach. The quantitative RT-PCR of ghrelin mRNA was assessed using the biopsy samples obtained by endoscopy at each site of the stomach (**a**). Ghrelin positive cells were counted by immunohistochemistry at each site of the stomach (**b**). There was an apparent correlation between ghrelin mRNA expression in gastric mucosa samples and ghrelin producing cell counts in immunohistochemistry ($R^2 = 0.87$, $P < 0.001$)

Discussion

This is the first study, which performed mapping and scoring of GPC in human subjects, focusing on the relationship between GPC and chronic gastritis using surgical samples of early gastric cancers. GPC has been known to be identical to the X/A-like cells in the fundic gland. Consistently, we observed GPC the most frequently in the great curvature in the upper body and fornix of the stomach where the fundic glands are well developed. Accompanying the progression of chronic gastritis, the number of GPC gradually decreased up to 10–20% of that without gastritis. The pattern of decline of GPC was various: some showed homogenous decrease of GPC in fundic gland area, but others showed heterogeneous or mosaic decrease, i.e. the GPC rich area was focally preserved. In general, GPC was well correlated with the preservation of fundic gland; however, we sometimes encountered the area where GPC was selectively lost despite when other components of fundic gland, such as chief cells and parietal cells, were present. Many clinical studies used endoscopic biopsy specimens for the evaluation of GPC. However, our observation might be a caution against these studies and we strongly recommend examining multiple specimens, at least one from the great curvature in the upper body and others from several lesions in fundic gland area.

The GPC score of the stomach was strongly correlated with serum ghrelin levels in the peripheral blood. This suggests the stomach is the main organ of ghrelin secretion and consistent with our previous observation that ghrelin has decreased to 10–20% after total gastrectomy [6, 7]. The current observation has also shown that the decline of GPC in the stomach was not compensated by the other ghrelin-producing organs, such as the duodenum, pancreas and hypothalamus, during the long history of chronic gastritis. With respect to the association with body weight, GPC score is not correlated with BMI, but serum ghrelin tends to negatively correlate with BMI in the GPC high group. This suggests the negative feedback that circulating ghrelin decrease in the obese individual was not by the regulation of GPC number but by that of the ghrelin secretion from GPC. GPC as well as serum ghrelin can be the surrogate marker of chronic gastritis like pepsinogen, gastrin and the presence of *H pylori*, while GPC might be more sensitive than serum ghrelin, since GPC is less influenced by body weight.

In this study, we used entire half stomach from patients with early gastric cancers, which should be good examples to investigate the relationship between chronic gastritis and ghrelin. The presence of cancer cells might not have much influence on GPC score and serum ghrelin levels, since the size of cancer nests was small and the GPC distribution was not perturbed in the mucosa surrounding the cancer nest. With respect to cancer cells, the high GPC group was associated with diffuse type cancers and low GPC group with intestinal type cancers. The association was considered due to the difference of background mucosa in each histological type. And it is unlikely that the ghrelin has a special effect on cancer progression. All the gastric cancer cells were negative for ghrelin immunohistochemistry in this study.

Ghrelin has acyl (active) and desacyl (inactive) forms and the active form accounts for 5.6–13% of total ghrelin [24]. Activation of ghrelin is conducted in the cytoplasm by ghrelin O-acyl transferase (GOAT), which is reported to co-exist with ghrelin in the stomach [25, 26]. However, the active form of ghrelin should be determined not only through the activation process by GOAT, but also through the inactivation by releasing the octanoyl-residue at Ser3 [24]. Ghrelin has a unique post-translational modification. The hydroxyl group of the third serine residue (Ser3) is esterified by octanoic acid and is essential for ghrelin's biological activities. The acyl modification of the hydroxyl group on the third residue represents an invariant and essential covalent change for the activation of ghrelin [24, 27]. Since the proportion of the active form varied among individuals and some conditions, it is quite interesting how the proportion of the active form and whether GOAT is constantly expressed in the GPC during the progression of chronic gastritis. We are planning further experiments with this issue.

Although this was an observational study with a small number of subjects, we can find important clues to resolve some surgical problems. Sleeve gastrectomy in bariatric surgery longitudinally removes the majority of the great curvature of the stomach. For successful body weight loss, not only gastric volume reduction but also appetite loss can be expected since the majority of GPC was removed by this procedure [28]. On the contrary, a gastric tube for reconstruction after esophagectomy was made of the great curvature of the stomach. Since body weight loss is a serious late complication after esophagectomy, preservation of the majority of GPC in the gastric tube might be beneficial to maintain the appetite. With respect to distal gastrectomy for gastric cancers, the majority of GPC should be anatomically preserved, but blood ghrelin decreases less than half [6, 7]. Vagotomy might be responsible for this discrepancy, therefore preservation of the vagal nerve might be worth attempting to maintain ghrelin and body weight.

Ghrelin, which plays a central role in the regulation of body weight and the appetite, should be a key molecule for studies of the various gastro-intestinal diseases, including chronic gastritis and morbid obesity. The precise distribution of GPC in the stomach is indispensable information for scientists and physicians and especially for the surgeon dealing with stomach.

Conclusion

This is the first study involving mapping of GPCs, which showed heterogenous impairment by chronic gastritis due to *H. pylori* infection. Since serum total ghrelin was mostly determined by the amount of GPCs and body weight, precise evaluation of GPCs should always be considered for the studies with respect to ghrelin.

Acknowledgments The authors thank Tomoyuki Sugimoto Ph.D. from the Department of Biomedical Statistics, Osaka University for advice on statistical analysis.

References

1. Kojima M, Hosoda H, Date Y, et al. Ghrelin is a growth-hormone-releasing acylated peptide from stomach. *Nature*. 1999;402:656–660.
2. Nakazato M, Murakami N, Date Y, et al. A role for ghrelin in the central regulation of feeding. *Nature*. 2001;409:194–198.
3. Masuda Y, Tanaka T, Inomata N, et al. Ghrelin stimulates gastric acid secretion and motility in rats. *Biochem Biophys Res Commun*. 2000;276:905–908.
4. Date Y, Kojima M, Nakazato M, et al. Ghrelin, a novel growth hormone-releasing acylated peptide, is synthesized in a distinct endocrine cell type in the gastrointestinal tracts of rats and humans. *Endocrinology*. 2000;141:4255–4261.
5. Leite-Moreira AF, Soares JB. Physiological, pathological and potential therapeutic roles of ghrelin. *Drug Discov Today*. 2007;12:276–288.
6. Takachi K, Doki Y, Ishikawa O, et al. Postoperative ghrelin levels and delayed recovery from body weight loss after distal or total gastrectomy. *J Surg Res*. 2006;130:1–7.
7. Doki Y, Takachi K, Ishikawa O, et al. Ghrelin reduction after esophageal substitution and its correlation to postoperative body weight loss in esophageal cancer patients. *Surgery*. 2006;139:797–805.
8. Simonsson M, Eriksson S, Håkanson R, et al. Endocrine cells in the human oxyntic mucosa. A histochemical study. *Scand J Gastroenterol*. 1988;23:1089–1099.
9. Shintani M, Watanabe M. Distribution of ghrelin-immunoreactive cells in human gastric mucosa: comparison with that of parietal cells. *J Gastroenterol*. 2005;40:345–349.
10. Osawa H, Nakazato M, Date Y, et al. Impaired production of gastric ghrelin in chronic gastritis associated with *Helicobacter pylori*. *J Clin Endocrinol Metab*. 2005;90:10–16.
11. Tatsuguchi A, Miyake K, Futagami S, et al. Effect of *Helicobacter pylori* on ghrelin expression in human gastric mucosa. *Am J Gastroenterol*. 2004;99:2121–2127.
12. Cummings DE, Weigle DS, Frayo RS, et al. Plasma ghrelin levels after diet-induced weight loss or gastric bypass surgery. *N Engl J Med*. 2002;346:1623–1630.
13. Ariyasu H, Takaya K, Tagami T, et al. Stomach is a major source of circulating ghrelin, and feeding state determines plasma

ghrelin-like immunoreactive levels in humans. *J Clin Endocrinol Metab*. 2001;86:4753–4758.
14. Isomoto H, Ueno H, Nishi Y, et al. Circulating ghrelin levels in patients with various upper gastrointestinal diseases. *Dig Dis Sci*. 2005;50:833.
15. Isomoto H, Ueno H, Saenko VA, et al. Impact of *Helicobacter pylori* infection on gastric and plasma ghrelin dynamics in humans. *Am J Gastroenterol*. 2005;100:1711–1720.
16. Inoue M, Tsugane S. Epidemiology of gastric cancer in Japan. *Postgrad Med J*. 2005;81:419–424.
17. Uemura N, Okamoto S, Yamamoto S, et al. Helicobacter pylori infection and the development of gastric cancer. *N Engl J Med*. 2001;345:784–789.
18. Kimura K, Takemoto T. An endoscopic recognition of the atrophic border and its significance in chronic gastritis. *Endoscopy*. 1969;3:87–97.
19. Kimura K, Satoh K, Ido K, et al. Gastritis in the Japanese stomach. *Scand J Gastroenterol Suppl*. 1996;214:17–20.
20. Hosoda H, Kojima M, Matsuo H, et al. Ghrelin and des-acyl ghrelin: two major forms of rat ghrelin peptide in gastrointestinal tissue. *Biochem Biophys Res Commun*. 2000;279:909–913.
21. Nagaya N, Kojima M, Uematsu M, et al. Hemodynamic and hormonal effects of human ghrelin in healthy volunteers. *Am J Physiol*. 2001;280:1483–1487.
22. Dixon MF, Genta RM, Yardley JH, et al. Classification and grading of gastritis. The updated Sydney System. International workshop on the histopathology of gastritis, Houston 1994. *Am J Surg Pathol*. 1996;20:1161–1181.
23. Gualillo O, Caminos J, Blanco M, et al. Ghrelin, a novel placental-derived hormone. *Endocrinology*. 2001;142:788–794.
24. Hosoda H, Kojima M, Kangawa K. Biological, physiological, and pharmacological aspects of ghrelin. *J Pharmacol Sci*. 2006;100:398–410.
25. Yang J, Brown MS, Liang G, et al. Identification of the acyltransferase the octanoylates ghrelin an appetite-stimulating peptide hormone. *Cell*. 2008;132:387–396.
26. Stengel A, Goebel M, Wang L, et al. Differential distribution of ghrelin-O-acyltransferase (GOAT) immunoreactive cells in the mouse and rat gastric oxyntic mucosa. *Biochem Biophys Res Commun*. 2010;392:67–71.
27. Kaiya H, Kojima M, Hosoda H, et al. Bullfrog ghrelin is modified by n-octanoic acid at its third threonine residue. *J Biol Chem*. 2001;276:40441–40448.
28. Karamanakos SN, Vagenas K, Kalfarentzos F, et al. Weight loss, appetite suppression, and changes in fasting and postprandial ghrelin and peptide-YY levels after Roux-en-Y gastric bypass and sleeve gastrectomy: a prospective, double blind study. *Ann Surg*. 2008;247:401–407.

Autonomic Neuroscience: Basic and Clinical 162 (2011) 60–65

Contents lists available at ScienceDirect

Autonomic Neuroscience: Basic and Clinical

journal homepage: www.elsevier.com/locate/autneu

Centrally administered ghrelin activates cardiac vagal nerve in anesthetized rabbits

Shuji Shimizu [a,b,*], Tsuyoshi Akiyama [a], Toru Kawada [a], Takashi Sonobe [a], Atsunori Kamiya [a], Toshiaki Shishido [a], Takeshi Tokudome [a], Hiroshi Hosoda [a], Mikiyasu Shirai [a], Kenji Kangawa [a], Masaru Sugimachi [a]

[a] National Cerebral and Cardiovascular Center Research Institute, Osaka, Japan
[b] Japan Association for the Advancement of Medical Equipment, Tokyo, Japan

ARTICLE INFO

Article history:
Received 30 June 2010
Received in revised form 8 March 2011
Accepted 6 April 2011

Keywords:
Ghrelin
Cardiac microdialysis
Norepinephrine
Acetylcholine
Vagal nerve

ABSTRACT

Although central ghrelin has cardioprotective effect through inhibiting sympathetic nerve activity, the effects of central ghrelin on cardiac vagal nerve remain unknown. We investigated the effects of centrally administered ghrelin on cardiac autonomic nerve activities using microdialysis technique. A microdialysis probe was implanted in the right atrial wall adjacent to the sinoatrial node of an anesthetized rabbit and was perfused with Ringer's solution containing a cholinesterase inhibitor, eserine. After injection of ghrelin (1 nmol) into the right lateral cerebral ventricle, norepinephrine (NE) and acetylcholine (ACh) concentrations in the dialysate samples were measured as indices of NE and ACh release from nerve endings to the sinoatrial node using high-performance liquid chromatography. Heart rate was 270 ± 4 bpm at baseline and decreased gradually after ghrelin injection to 234 ± 9 bpm ($P<0.01$) at 60–80 min, followed by gradual recovery. Dialysate ACh concentration was 5.5 ± 0.8 nM at baseline and increased gradually after ghrelin injection to 8.8 ± 1.2 nM ($P<0.01$) at 60–80 min; the concentration started to decrease gradually from 100 to 120 min after injection reaching 5.6 ± 0.8 nM at 160–180 min. Central ghrelin did not change mean arterial pressure or dialysate NE concentration. The elevated dialysate ACh concentration declined rapidly after transection of cervical vagal nerves. These results indicate that centrally administered ghrelin activates cardiac vagal nerve.

1. Introduction

Ghrelin, a growth-hormone-releasing acylated peptide, was originally isolated from rat stomach (Kojima et al., 1999). Immunohistochemical studies have revealed that ghrelin-immunoreactive neurons are also present in the central nervous system including the hypothalamic arcuate nucleus (ARC) (Date et al., 2000) and that growth hormone secretagogue receptors (GHS-R) are expressed in hypothalamic nucleus including the ARC (Guan et al., 1997). Several studies have demonstrated that centrally administered ghrelin inhibits sympathetic nerve activity. Matsumura et al. (2002) reported that intracerebroventricular (icv) injection of ghrelin decreased renal sympathetic nerve activity in conscious rabbits. Lin et al. (2004) showed that microinjection of ghrelin into the nucleus of the solitary tract (NTS) also suppressed the renal sympathetic nerve activity in rats. However, whether central ghrelin affects cardiac vagal nerve activity remains unknown. Recently we have developed a microdialysis technique that allows direct monitoring of norepinephrine (NE) and acetylcholine (ACh) released into the sinoatrial (SA) node (Shimizu et al., 2009, 2010). Dialysate NE or ACh concentration monitored by this technique significantly correlates with heart rate and the frequencies of electrical stimulation of sympathetic or vagal nerve. In the present study, we used this technique to investigate the effect of centrally administered ghrelin on cardiac vagal nerve activity as well as sympathetic nerve activity in anesthetized rabbits.

2. Materials and Methods

2.1. Surgical Preparation

Animal care was provided in accordance with the *Guiding Principles for the Care and Use of Animals in the Field of Physiological Sciences* approved by the Physiological Society of Japan. All protocols were approved by the Animal Subject Committee of the National Cerebral and Cardiovascular Center. Twenty four Japanese white rabbits weighing 2.3 to 3.1 kg were used in this study. Anesthesia was initiated by an intravenous injection of pentobarbital sodium (50 mg/kg) via the marginal ear vein, and then maintained at an appropriate level by continuous intravenous infusion of α-chloralose (16 mg/kg/h) and urethane (100 mg/kg/h) through a catheter inserted into the femoral vein. Since the duration of this experiment was projected to be over 8 h, the animals were intubated and ventilated mechanically with room air mixed with oxygen. Respiratory rate and tidal volume were set at

* Corresponding author at: Department of Cardiovascular Dynamics, National Cerebral and Cardiovascular Center Research Institute, 5-7-1 Fujishiro-dai, Suita, Osaka 565-8565, Japan. Tel.: +81 6 6833 5012; fax: +81 6 6835 5403.
E-mail address: shujismz@ri.ncvc.go.jp (S. Shimizu).

1566-0702/$ – see front matter © 2011 Elsevier B.V. All rights reserved.
doi:10.1016/j.autneu.2011.04.001

30 cycles/min and 15 ml/kg, respectively. Systemic arterial pressure was monitored by a catheter inserted into the femoral artery. Body temperature was measured in the esophagus by a thermometer (CTM-303, Terumo, Japan), and was maintained between 38 and 39 °C using a heating pad. For icv injection of ghrelin, a polyethylene tube (500 μm outer diameter) was stereotactically inserted into the right lateral cerebral ventricle using a guiding needle (900 μm outer diameter, 600 μm inner diameter) and was perfused continuously with artificial cerebrospinal fluid (CSF) solution (ARTCEREB®, Otsuka, Japan) at a rate of 2 μl/min using a microinjection pump (CMA/102, Carnegie Medicin, Sweden).

With the animal in the lateral position, right lateral thoracotomy was performed and the right 3rd to 5th ribs were partially resected to expose the heart. Three stainless electrodes were placed around the thoracotomy incision to record the body surface electrocardiogram. The heart rate was determined from the electrocardiogram using a cardiotachometer. Heparin sodium (100 IU/kg) was administered intravenously to prevent blood coagulation. A dialysis probe was implanted and dialysis was conducted as described in *Dialysis Technique* below. At the end of the experiment, the animal was euthanized by injecting an overdose of pentobarbital sodium. In the postmortem examination, the right atrial wall with the implanted dialysis fiber was resected. The endocardial side of atrial wall was examined macroscopically to confirm that the dialysis membrane was not exposed to the right atrial lumen.

2.2. Dialysis Technique

The materials and properties of the dialysis probe have been described previously (Akiyama et al., 1991; Shimizu et al., 2009, 2010). A dialysis fiber composed of semipermeable membrane (4 mm length, 310 μm outer diameter, 200 μm inner diameter; PAN-1200, 50,000 molecular weight cutoff; Asahi Chemical, Tokyo, Japan) was attached at both ends to polyethylene tubes (25 cm length, 500 μm outer diameter, 200 μm inner diameter). A fine guiding needle (30 mm length, 510 μm outer diameter, 250 μm inner diameter) with a stainless steel rod (5 mm length, 250 μm outer diameter) was used for implantation. A dialysis probe was implanted into the right atrial myocardium near the junction between the superior vena cava and the right atrium. After implantation, the dialysis probe was perfused with Ringer's solution (NaCl 147 mM, KCl 4 mM, and $CaCl_2$ 3 mM) containing the cholinesterase inhibitor, eserine (100 μM), at a rate of 2 μl/min using a microinjection pump (CMA/102). Experimental protocols were started 120 min after implantation of the dialysis probe. We took account of the dead space between the dialysis membrane and the sample tube at the start of each dialysate sampling. Eight microliters of phosphate buffer (pH 3.5) was added to each sample tube before dialysate sampling. The duration of dialysate sampling was fixed at 20 min (1 sample volume = 40 μl). Half of the dialysate sample was used for ACh measurement and the other half for NE. Dialysate NE and ACh concentrations were measured separately using two high-performance liquid chromatographs with electrochemical detection as previously described (Akiyama et al., 1991, 1994).

2.3. Experimental Protocols

2.3.1. Protocol 1

We investigated the time courses of heart rate, mean arterial pressure, and dialysate NE and ACh concentrations following icv injection of ghrelin. One hundred microliters of artificial CSF containing 1 nmol of human ghrelin (Peptide Institute, Osaka, Japan) or 100 μl of artificial CSF alone (vehicle) was injected into the lateral cerebral ventricle of a rabbit. Baseline dialysate sample was collected before injection and then 20-min dialysate samples were collected consecutively up to 180 min after injection.

2.3.2. Protocol 2

We investigated the effect of vagotomy on heart rate and cardiac vagal ACh release after icv injection of ghrelin (1 nmol). Baseline dialysate sample was collected before icv injection of ghrelin and another sample was collected when heart rate reached a trough after ghrelin injection. Immediately after this sampling, bilateral cervical vagal nerves were transected and dialysate was sampled for a 20-min duration.

2.3.3. Protocol 3

As a supplemental protocol, we investigated the dose-dependent effects of ghrelin on heart rate and dialysate ACh concentration using icv injection of 0.2 nmol ($n=3$) or 5 nmol ($n=4$) of human ghrelin into the right lateral cerebral ventricle. Baseline dialysate sample was collected before injection and then 20-min dialysate samples were collected consecutively up to 180 min after injection.

2.4. Statistical analysis

Heart rate and mean arterial pressure were averaged over each 20-min duration of dialysate sampling. All data are presented as mean ± SE. In Protocols 1 and 2, heart rate and mean arterial pressure were compared by one-way repeated measures analysis of variance (ANOVA) followed by a Dunnett's test against baseline. Our previous studies demonstrated that dialysate NE or ACh concentration exponentially increased in response to electrical stimulation of sympathetic or vagal nerve. Then, heart rate linearly correlated with logarithms of dialysate NE or ACh concentration (Shimizu et al., 2009, 2010). Thus, after logarithmic transformation, dialysate NE and ACh concentrations were compared by one-way repeated measures ANOVA followed by a Dunnett's test against baseline. The differences between ghrelin and vehicle groups were compared using unpaired *t*-test. Differences were considered significant at $P<0.05$.

3. Results

3.1. Protocol 1

In the ghrelin-treated rabbits, the heart rate was 270 ± 4 bpm at baseline and decreased gradually after icv ghrelin injection reaching a trough of 233 ± 9 bpm at 80–100 min ($P<0.01$ vs. baseline), followed by gradual recovery (271 ± 8 bpm at 160–180 min). In the vehicle control group, heart rate was 270 ± 6 bpm at baseline and increased slightly to 278 ± 6 bpm at 40–60 min after injection ($P<0.05$ vs. baseline), and was maintained until the end of the protocol (284 ± 7 bpm at the 160–180 min, $P<0.01$ vs. baseline) (Fig. 1A).

Although mean arterial pressure did not change after icv injection of ghrelin and remained constant throughout the experiment, mean arterial pressure decreased gradually from 80 ± 4 mm Hg at baseline to 72 ± 2 mm Hg at 160–180 min ($P<0.01$ vs. baseline) after icv injection of vehicle (Fig. 1B).

Dialysate ACh concentration did not change after icv injection of vehicle. In the ghrelin-treated rabbits, the dialysate ACh concentration was 5.5 ± 0.8 nM at baseline and increased gradually after ghrelin injection, reaching a plateau of 8.8 ± 1.2 nM at 60–80 min ($P<0.01$ vs. baseline). The concentration appeared to decline after 100 min and returned to 5.6 ± 0.8 nM at 160–180 min (N.S. vs. baseline) (Fig. 2A).

Dialysate NE concentration did not change after icv injection of ghrelin or vehicle, and did not vary significantly throughout the experiment (Fig. 2B).

3.2. Protocol 2

Heart rate decreased significantly from 283 ± 5 bpm at baseline to a trough of 249 ± 5 bpm after icv injection of ghrelin ($P<0.01$ vs. baseline) (Table 1). Dialysate ACh concentration increased from 5.3 ± 1.3 nM at

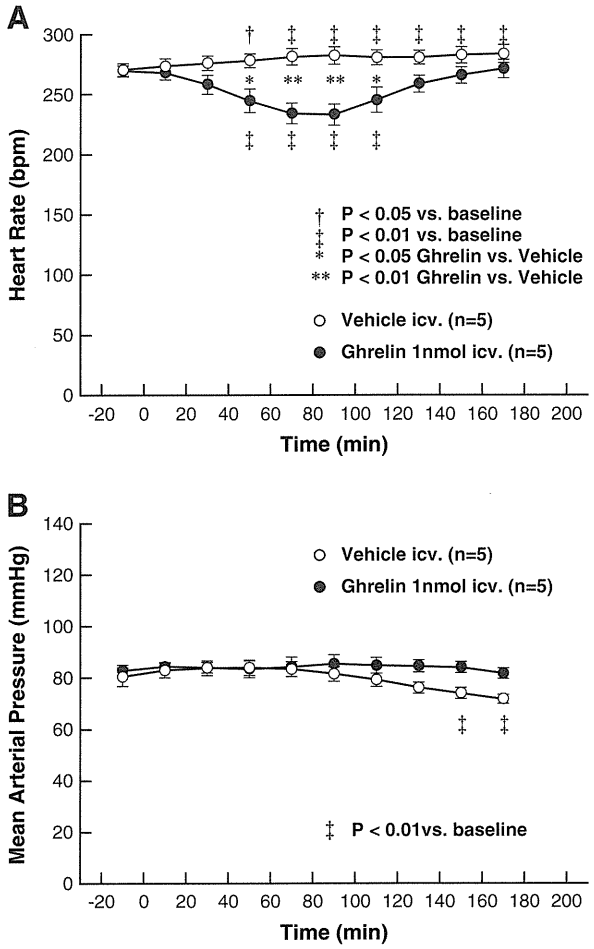

Fig. 1. Time courses of heart rate (A) and mean arterial pressure (B) elicited by intracerebroventricular (icv) injection of 1 nmol of ghrelin (●) or artificial cerebrospinal fluid (vehicle, ○) (n = 5 in each group). Data are presented as values averaged over each 20-min duration of dialysate sampling. Values are mean ± SE. † P<0.05, ‡ P<0.01 vs. baseline before injection by one-way repeated measures analysis of variance followed by Dunnett's test. * P<0.05, ** P<0.01 ghrelin vs. vehicle by unpaired *t*-test.

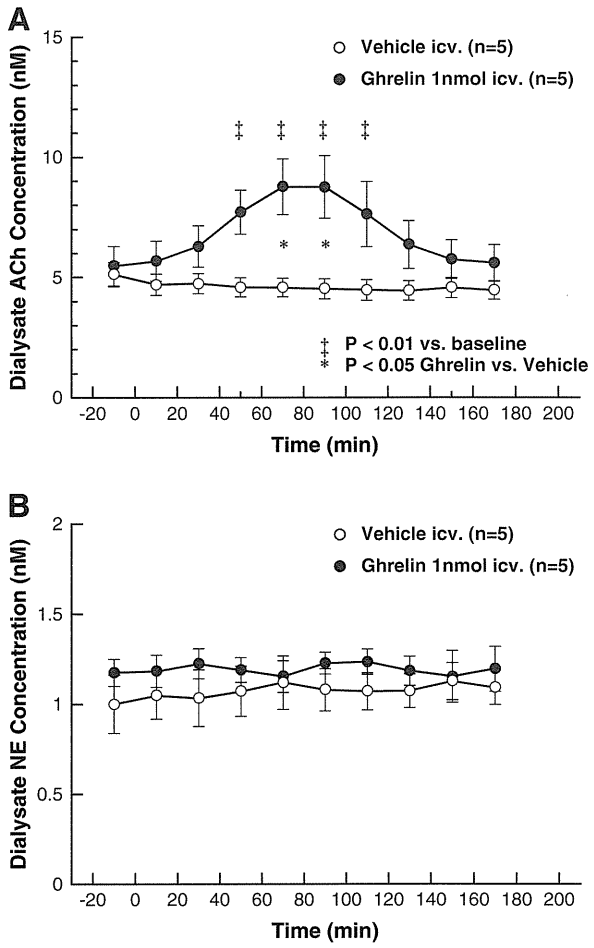

Fig. 2. Time courses of dialysate acetylcholine (ACh) (A) and norepinephrine (NE) (B) concentrations elicited by icv injection of ghrelin (●) or vehicle (○) (n = 5 in each group). Data are concentrations in dialysate samples collected over 20-min durations. Values are mean ± SE. Statistical comparison was performed after logarithmic transformation. ‡ P<0.01 vs. baseline before injection by one-way repeated measures analysis of variance followed by Dunnett's test. * P<0.05, ghrelin vs. vehicle by unpaired *t*-test.

baseline to 9.5 ± 2.2 nM at the time of trough heart rate after icv ghrelin injection (P<0.01 vs. baseline) (Fig. 3A). After vagotomy, heart rate immediately increased to 286 ± 8 bpm (N.S. vs. baseline) and mean arterial pressure decreased to 76 ± 9 mm Hg (P<0.05 vs. baseline), while dialysate ACh concentration recovered to the baseline level (6.6 ± 1.9 nM, N.S. vs. baseline). Typical heart rate response after vagotomy is shown in Fig. 3B.

3.3. Protocol 3

Heart rate decreased from 272 ± 15 bpm at baseline to 209 ± 29 bpm at 80–100 min after icv injection of 5 nmol of ghrelin (Fig. 4A). Dialysate ACh concentration increased from 6.4 ± 1.2 nM at baseline to 11.2 ± 1.7 nM at 80–100 min after icv injection of 5 nmol of ghrelin (Fig. 4B). At the end of this experiment, heart rate was still lower (224 ± 23 bpm) than the baseline heart rate and dialysate ACh concentration was still higher (9.1 ± 0.9 nM) than that of baseline. Statistical analysis on these data was avoided due to the limited number of animals in the supplemental protocol.

Heart rate and dialysate ACh concentration did not change perceivably after icv injection of 0.2 nmol of ghrelin (Fig. 4A and B).

4. Discussion

The major finding of the present study is that centrally administered ghrelin increases ACh release into the SA node by activating efferent cardiac vagal nerves.

4.1. Ghrelin and cardiac vagal nerve activity

Intracerebroventricular injection of ghrelin is known to activate efferent vagal nerves in digestive organs. Li et al. (2006) and Sato et al. (2003) have

Table 1
Changes in heart rate and mean arterial pressure after intracerebroventricular injection of 1 nmol of ghrelin followed by vagotomy.

	Heart rate (bpm)	Mean arterial pressure (mm Hg)
Baseline (before injection)	283 ± 5	82 ± 7
Trough level after injection (before vagotomy)	249 ± 5**	79 ± 8
After vagotomy	286 ± 8	76 ± 9*

Values are mean ± SE (n = 7).
* P<0.05 vs. baseline.
** P<0.01 vs. baseline.

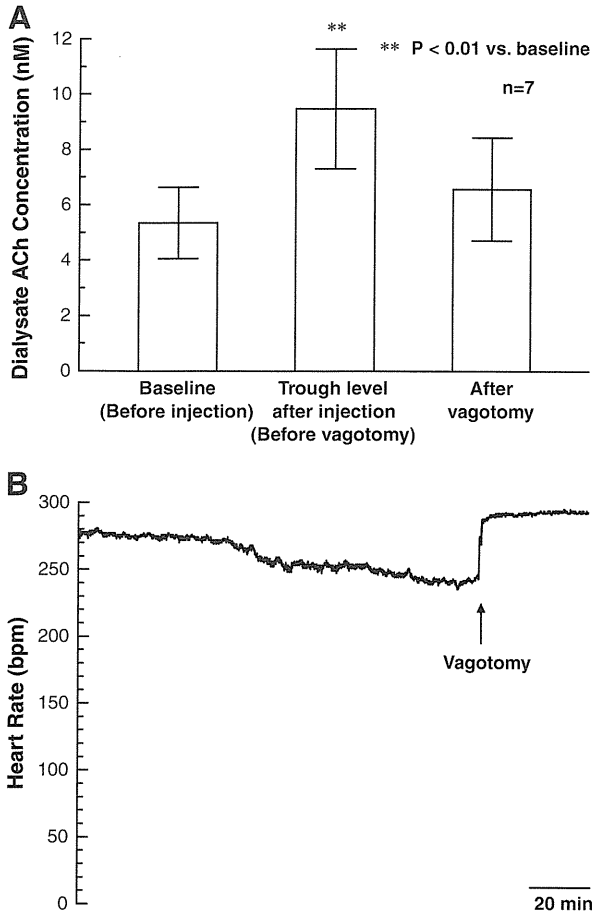

Fig. 3. A: Effect of vagotomy after icv injection of 1 nmol of ghrelin on dialysate ACh concentration (n = 7). Values are mean ± SE. Statistical comparison was performed after logarithmic transformation. ** P<0.01 vs. baseline before injection by one-way repeated measures analysis of variance followed by Dunnett's test. B: Typical time course of heart rate change. Heart rate gradually decreased after icv injection of ghrelin and promptly returned to the baseline level after vagatomy.

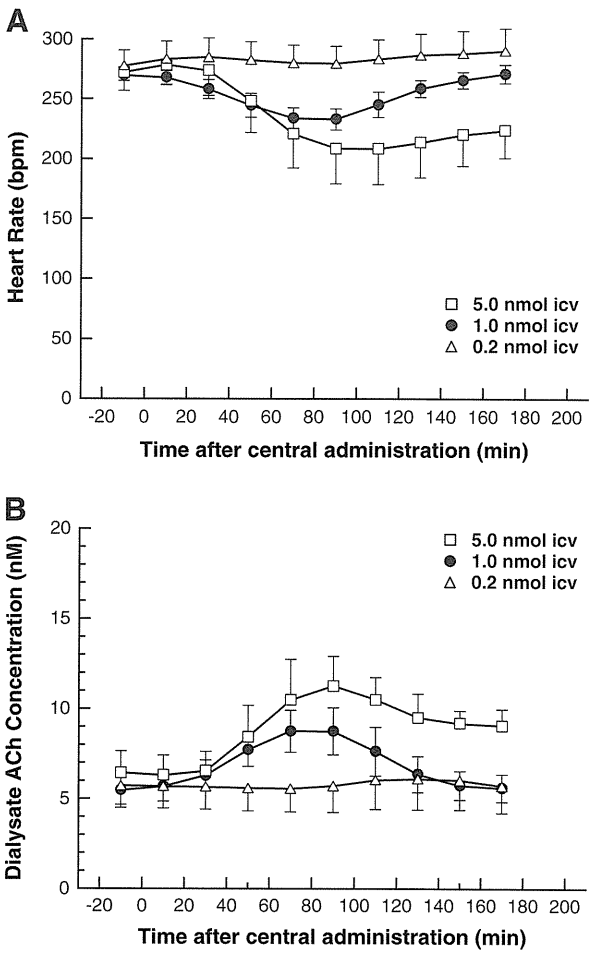

Fig. 4. Time courses of heart rate (A) and dialysate ACh concentration (B) elicited by icv injection of 0.2 nmol (△, n = 3) or 5 nmol (□, n = 4) of ghrelin. Graphs of icv injection of 1 nmol of ghrelin (●) were reproduced from Figs. 1A and 2A for intuitive comparison.

demonstrated that icv injection of ghrelin stimulates pancreatic secretion by activating efferent vagal nerves. Kobashi et al. (2009) have shown that icv injection of ghrelin induces relaxation of the proximal stomach through activation of efferent vagal nerves. Vagal nerves also play an important role in the regulation of heart rate under physiological conditions. Moreover, vagal stimulation has cardioprotective effect against chronic heart failure (Li et al., 2004; Schwartz et al., 2008). However, the effect of icv injection of ghrelin on cardiac vagal nerve activity has not been reported.

In the present study, icv injection of ghrelin decreased heart rate without affecting mean arterial pressure, and simultaneously increased dialysate ACh concentration without changing dialysate NE concentration. The time course of heart rate changes parallels that of dialysate ACh concentration changes throughout the experiment. Furthermore, dialysate ACh concentration and heart rate recovered to the baseline levels immediately after vagotomy. Thus, the decrease in heart rate by central ghrelin could be due to cardiac vagal activation and not cardiac sympathetic suppression. The present study demonstrates that centrally administered ghrelin activates cardiac vagal nerve and decreases heart rate. The maximal dialysate ACh concentration following icv injection of ghrelin reached 8.8 ± 1.2 nM. This dialysate ACh concentration is almost equivalent to that induced by electrical stimulation of the right cervical vagal nerve at 10–20 Hz (Shimizu et al., 2009). Therefore, ghrelin may be one of the most important mediators in the central nerve system, which activates cardiac vagal nerve.

Ghrelin receptors are present in the central nerve system. In a c-Fos expression study, Date et al. (2001) reported that central ghrelin activated the NTS and dorsal motor nucleus of the vagus (DMNV). Zigman et al. (2006) demonstrated the presence of GHS-R in all three divisions of the dorsal vagal complex using in situ hybridization. The GHS-Rs are also expressed in the hypothalamus including the ARC (Guan et al., 1997). Central administration of ghrelin may activate cardiac vagal nerve through direct action on central ghrelin receptors, although it is difficult to determine the brain region in which ghrelin acts from the present study.

There was a long time lag between icv injection of ghrelin and activation of the cardiac vagal nerve. This may suggest that other mediators are involved in ghrelin-induced activation of cardiac vagal nerve. Intracerebroventricular injection of ghrelin evokes growth hormone release (Date et al., 2000). Resmini et al. (2006) reported sympathovagal imbalance due to vagal hypertone in acromegalic patients. Sato et al. (2003), however, suggested that the stimulatory effect of ghrelin on pancreatic secretion may be induced independent of its growth-hormone releasing effect, because a maximal increase in growth hormone was observed 10–20 min after ghrelin injection but a peak increase in pancreatic secretion was found 30–60 min after injection. In the present study, the maximal decrease in heart rate (234 ± 9 and 233 ± 9 bpm) and maximal increase in dialysate ACh concentration (8.8 ± 1.2 and 8.7 ± 1.3 nM) were both observed during 60–100 min after icv ghrelin injection. Moreover, Bisi et al. (1999) reported that intravenous administration of recombinant human growth hormone increased circulating growth hormone levels but did

not affect heart rate or mean arterial pressure in humans. Therefore, the stimulatory effect of ghrelin on the cardiac vagal nerve may be independent of its growth hormone releasing effect.

Nakazato et al. (2001) reported that antibodies and antagonists of neuropeptide Y and agouti-related protein abolished ghrelin-enhanced feeding. Kamegai et al. (2001) reported that chronic icv infusion of ghrelin increased both neuropeptide Y and agouti-related protein mRNA levels in the ARC. Moreover, Kobashi et al. (2006) showed that central neuropeptide Y induced proximal stomach relaxation via Y1 receptors in the dorsal vagal complex of rats. Thus, neuropeptide Y and agouti-related protein may be involved in the stimulatory effect of ghrelin on cardiac vagal nerve. However, we need further investigations to identify the mediators involved in the ghrelin-induced cardiac vagal activation.

4.2. Ghrelin and cardiac sympathetic nerve activity

In the present study, icv injection of ghrelin did not change dialysate NE concentration. This result indicates that centrally administered ghrelin did not affect NE release into the SA node under the present experimental conditions. Central ghrelin has been shown to inhibit sympathetic nerve activity in conscious rabbits (Matsumura et al., 2002). The present study was performed under anesthetized conditions. The difference in effect on sympathetic nerve activity may be related to experimental conditions including anesthesia and artificial ventilation. Schwenke et al. (2008) reported that subcutaneous administration of ghrelin prevented the increase in cardiac sympathetic nerve activity in the acute phase after myocardial infarction. Soeki et al. (2008) also reported that sympathetic nerve activity was inhibited by subcutaneous administration of ghrelin in rats with myocardial infarction, but not in sham-operated rats. Ghrelin seems to have a stronger inhibitory effect on the activated sympathetic nervous system than on the non-activated system. The basal sympathetic tone under our experimental conditions may not have been sufficiently high to reveal the sympathoinhibitory effect of ghrelin.

The basal vagal tone could also affect the sympathoinhibitory effect of ghrelin. Lin et al. (2004) reported that microinjection of ghrelin into the NTS did not affect heart rate and reduced the response of mean arterial pressure after intravenous administration of atropine sulfate. Thus, the vagal nerve may play an important role in ghrelin-induced sympathetic suppression. The sympathoinhibitory effect of ghrelin may be partly dependent on prejunctional inhibition of NE release via muscarinic receptors associated with vagal nerve activation. In Lin's study, however, depressor response of ghrelin appeared even after atropine treatment. Thus, it is highly possible that centrally administered ghrelin has a certain sympathoinhibitory effect. We need further investigations about the sympathoinhibitory effect of ghrelin.

4.3. Methodological considerations

First, ACh is degraded by ACh esterase immediately after its release. To monitor ACh release in vivo, addition of an ACh esterase inhibitor (eserine) into the perfusate is required. In our previous study, dialysate ACh concentration correlated well with heart rate and the frequency of cervical vagal nerve stimulation in the presence of eserine (Shimizu et al., 2009). Therefore, the increase in dialysate ACh concentration by icv injection of ghrelin should reflect the activation of cardiac vagal nerve even in the presence of eserine.

Second, the eserine can also affect NE release from sympathetic nerve endings as follows. The eserine should spread around the semipermeable membrane, thereby affecting the NE release in the vicinity of the semipermeable membrane through the enhancement of muscarinic receptor mediated prejunctional inhibition.

Third, to detect changes in dialysate NE and ACh concentration sampled from the right atrium, cardiac microdialysis technique requires 20-min sampling duration. The temporal resolution may be still insufficient compared to acute changes in hemodynamics such as that observed after vagotomy in Protocol 2. The improvement of sensitivity of liquid chromatography will lead to higher temporal resolution of this technique.

Fourth, in the present study, animals were in the supine position during dialysate sampling because this experiment was performed at open-chest condition for cardiac microdialysis. The supine position may have delayed the diffusion of ghrelin and prolonged the time-lag between the injection and vagal nerve activation. Thus, the position of animals may affect the time course of hemodynamics.

4.4. Conclusion

Using cardiac microdialysis technique, we demonstrated that centrally administered ghrelin was able to activate cardiac vagal nerve. Central ghrelin may play an important role in vagal cardiovascular control.

Acknowledgments

This study was supported by the research project promoted by Ministry of Health, Labour and Welfare in Japan (H20-katsudo-Shitei-007, H21-nano-ippan-005), the Grants-in-Aid for Scientific Research promoted by Ministry of Education, Culture, Sports, Science and Technology in Japan (#20390462 and #20590242) and the Industrial Technology Research Grant Program from New Energy and Industrial Technology Development Organization (NEDO) of Japan.

References

Akiyama, T., Yamazaki, T., Ninomiya, I., 1991. In vivo monitoring of myocardial interstitial norepinephrine by dialysis technique. Am. J. Physiol. 261, H1643–H1647.
Akiyama, T., Yamazaki, T., Ninomiya, I., 1994. In vivo detection of endogenous acetylcholine release in cat ventricles. Am. J. Physiol. 266, H854–H860.
Bisi, G., Podio, V., Valetto, M.R., Broglio, F., Bertuccio, G., Del Rio, G., Arvat, E., Boghen, M.F., Deghenghi, R., Muccioli, G., Ong, H., Ghigo, E., 1999. Acute cardiovascular and hormonal effects of GH and hexarelin, a synthetic GH-releasing peptide, in humans. J. Endocrinol. Invest. 22, 266–272.
Date, Y., Murakami, N., Kojima, M., Kuroiwa, T., Matsukura, S., Kangawa, K., Nakazato, M., 2000. Central effects of a novel acylated peptide, ghrelin, on growth hormone release in rats. Biochem. Biophys. Res. Commun. 275, 477–480.
Date, Y., Nakazato, M., Murakami, N., Kojima, M., Kangawa, K., Matsukura, S., 2001. Ghrelin acts in the central nervous system to stimulate gastric acid secretion. Biochem. Biophys. Res. Commun. 280, 904–907.
Guan, X.M., Yu, H., Palyha, O.C., McKee, K.K., Feighner, S.D., Sirinathsinghji, D.J., Smith, R.G., Van der Ploeg, L.H., Howard, A.D., 1997. Distribution of mRNA encoding the growth hormone secretagogue receptor in brain and peripheral tissues. Brain Res. Mol. Brain Res. 48, 23–29.
Kamegai, J., Tamura, H., Shimizu, T., Ishii, S., Sugihara, H., Wakabayashi, I., 2001. Chronic central infusion of ghrelin increases hypothalamic neuropeptide Y and Agouti-related protein mRNA levels and body weight in rats. Diabetes 50, 2438–2443.
Kobashi, M., Shimatani, Y., Shirota, K., Xuan, S.Y., Mitoh, Y., Matsuo, R., 2006. Central neuropeptide Y induces proximal stomach relaxation via Y1 receptors in the dorsal vagal complex of the rat. Am. J. Physiol. Regul. Integr. Comp. Physiol. 290, R290–R297.
Kobashi, M., Yanagihara, M., Fujita, M., Mitoh, Y., Matsuo, R., 2009. Fourth ventricular administration of ghrelin induces relaxation of the proximal stomach in the rat. Am. J. Physiol. Regul. Integr. Comp. Physiol. 296, R217–R223.
Kojima, M., Hosoda, H., Date, Y., Nakazato, M., Matsuo, H., Kangawa, K., 1999. Ghrelin is a growth-hormone-releasing acylated peptide from stomach. Nature 402, 656–660.
Li, M., Zheng, C., Sato, T., Kawada, T., Sugimachi, M., Sunagawa, K., 2004. Vagal nerve stimulation markedly improves long-term survival after chronic heart failure in rats. Circulation 109, 120–124.
Li, Y., Wu, X., Zhao, Y., Chen, S., Owyang, C., 2006. Ghrelin acts on the dorsal vagal complex to stimulate pancreatic protein secretion. Am. J. Physiol. Gastrointest. Liver Physiol. 290, G1350–G1358.
Lin, Y., Matsumura, K., Fukuhara, M., Kagiyama, S., Fujii, K., Iida, M., 2004. Ghrelin acts at the nucleus of the solitary tract to decrease arterial pressure in rats. Hypertension 43, 977–982.
Matsumura, K., Tsuchihashi, T., Fujii, K., Abe, I., Iida, M., 2002. Central ghrelin modulates sympathetic activity in conscious rabbits. Hypertension 40, 694–699.
Nakazato, M., Murakami, N., Date, Y., Kojima, M., Matsuo, H., Kangawa, K., Matsukura, S., 2001. A role for ghrelin in the central regulation of feeding. Nature 409, 194–198.
Resmini, E., Casu, M., Patrone, V., Murialdo, G., Bianchi, F., Giusti, M., Ferone, D., Minuto, F., 2006. Sympathovagal imbalance in acromegalic patients. J. Clin. Endocrinol. Metab. 91, 115–120.

Sato, N., Kanai, S., Takano, S., Kurosawa, M., Funakoshi, A., Miyasaka, K., 2003. Central administration of ghrelin stimulates pancreatic exocrine secretion via the vagus in conscious rats. Jpn. J. Physiol. 53, 443–449.
Schwartz, P.J., De Ferrari, G.M., Sanzo, A., Landolina, M., Rordorf, R., Raineri, C., Campana, C., Revera, M., Ajmone-Marsan, N., Tavazzi, L., Odero, A., 2008. Long term vagal stimulation in patients with advanced heart failure: first experience in man. Eur. J. Heart Fail. 10, 884–891.
Schwenke, D.O., Tokudome, T., Kishimoto, I., Horio, T., Shirai, M., Cragg, P.A., Kangawa, K., 2008. Early ghrelin treatment after myocardial infarction prevents an increase in cardiac sympathetic tone and reduces mortality. Endocrinology 149, 5172–5176.
Shimizu, S., Akiyama, T., Kawada, T., Shishido, T., Yamazaki, T., Kamiya, A., Mizuno, M., Sano, S., Sugimachi, M., 2009. In vivo direct monitoring of vagal acetylcholine release to the sinoatrial node. Auton. Neurosci. 148, 44–49.
Shimizu, S., Akiyama, T., Kawada, T., Shishido, T., Mizuno, M., Kamiya, A., Yamazaki, T., Sano, S., Sugimachi, M., 2010. In vivo direct monitoring of interstitial norepinephrine levels at the sinoatrial node. Auton. Neurosci. 152, 115–118.
Soeki, T., Kishimoto, I., Schwenke, D.O., Tokudome, T., Horio, T., Yoshida, M., Hosoda, H., Kangawa, K., 2008. Ghrelin suppresses cardiac sympathetic activity and prevents early left ventricular remodeling in rats with myocardial infarction. Am. J. Physiol. Heart Circ. Physiol. 294, H426–H432.
Zigman, J.M., Jones, J.E., Lee, C.E., Saper, C.B., Elmquist, J.K., 2006. Expression of ghrelin receptor mRNA in the rat and the mouse brain. J. Comp. Neurol. 494, 528–548.

Pflugers Arch - Eur J Physiol (2011) 462:397–406
DOI 10.1007/s00424-011-0992-8

CARDIOVASCULAR PHYSIOLOGY

Exogenous ghrelin improves blood flow distribution in pulmonary hypertension—assessed using synchrotron radiation microangiography

Daryl O. Schwenke · Emily A. Gray · James T. Pearson · Takashi Sonobe · Hatsue Ishibashi-Ueda · Isabel Campillo · Kenji Kangawa · Keiji Umetani · Mikiyasu Shirai

Received: 12 April 2011 / Revised: 9 June 2011 / Accepted: 23 June 2011 / Published online: 9 July 2011

Abstract Ghrelin has cardioprotective properties and, recently, has been shown to improve endothelial function and reduce endothelin-1 (ET-1)-mediated vasoconstriction in peripheral vascular disease. Recently, we reported that ghrelin attenuates pulmonary hypertension (PH) caused by chronic hypoxia (CH), which we hypothesized in this study may be via suppression of the ET-1 pathway. We also aimed to determine whether ghrelin's ability to prevent alterations of the ET-1 pathway also prevented adverse changes in pulmonary blood flow distribution associated with PH. Sprague–Dawley rats were exposed to CH (10% O_2 for 2 weeks) with daily subcutaneous injections of ghrelin (150 μg/kg) or saline. Utilizing synchrotron radiation microangiography, we assessed pulmonary vessel branching structure, which is indicative of blood flow distribution, and dynamic changes in vascular responsiveness to (1) ET-1 (1 nmol/kg), (2) the $ET\text{-}1_A$ receptor antagonist, BQ-123 (1 mg/kg), and (3) ACh (3.0 μg kg^{-1} min^{-1}). CH impaired blood flow distribution throughout the lung. However, this vessel "rarefaction" was attenuated in ghrelin-treated CH-rats. Moreover, ghrelin (1) reduced the magnitude of endothelial dysfunction, (2) prevented an increase in ET-1-mediated vasoconstriction, and (3) reduced pulmonary vascular remodeling and right ventricular hypertrophy—all adverse consequences associated with CH. These results highlight the beneficial effects of ghrelin for maintaining optimal lung perfusion in the face of a hypoxic insult. Further research is now required to establish whether ghrelin is also an effective therapy for restoring normal pulmonary hemodynamics in patients that already have established PH.

Keywords Ghrelin · Chronic hypoxia · Pulmonary hypertension · Endothelin-1 · Rat

D. O. Schwenke (✉) · E. A. Gray · I. Campillo
Department of Physiology, University of Otago,
PO Box 56, Dunedin, New Zealand
e-mail: daryl.schwenke@otago.ac.nz

J. T. Pearson
Department of Physiology, Monash University,
Melbourne, Australia

J. T. Pearson
Australian Synchrotron,
Melbourne, Australia

T. Sonobe · M. Shirai
Department of Cardiac Physiology,
National Cerebral and Cardiovascular Center Research Institute,
Suita, Osaka, Japan

H. Ishibashi-Ueda
Department of Pathology,
National Cerebral and Cardiovascular Center Research Institute,
Suita, Osaka, Japan

K. Kangawa
National Cardiovascular Center Research Institute,
Suita, Osaka, Japan

K. Umetani
Japan Synchrotron Radiation Research Institute,
Sayo-gun, Hyogo, Japan

Introduction

Several pulmonary pathologies are typically associated with adverse chronic alveolar hypoxia, which consequently elevates pulmonary arterial pressure (PAP) culminating in the development of pulmonary hypertension (PH).

Unfortunately, there is still no effective cure for PH, which is associated with high mortality. Over the last decade, it has become apparent that dysfunction of the pulmonary vascular endothelium acts as a fundamental trigger for instigating the pathogenesis of PH. Indeed, disruption of the pathways for specific vascular vasoactive substances, such as endothelin-1 (ET-1) [11, 12, 31] and nitric oxide (NO) [1, 6, 7, 15] contribute to the pathogenesis of PH. Of interest, ET-1 is a potent vasoconstrictor released from the pulmonary vascular endothelium and plays a pivotal role in modulating pulmonary vascular tone.

Ever since its discovery in 1999 [13], ghrelin has been implicated in a diverse range of physiological functions (see review [14]). Recently, we reported that exogenous ghrelin administration was able to attenuate the magnitude of PH in rats exposed to chronic hypoxia (CH) [23]. We also proposed that this therapeutic effect may be linked to ghrelin's ability to prevent an over-expression of ET-1 within the pulmonary vasculature of chronic hypoxic rats, based on previous reports showing that ghrelin could antagonize the vasoconstrictor effects of ET-1 [28].

Although these findings highlight the therapeutic potential of ghrelin for PH, one fundamental limitation is that this study failed to establish whether ghrelin is able to maintain "normal" blood flow distribution throughout the lung during the development of PH. Indeed, pulmonary rarefaction (i.e., vessel pruning) and extensive vascular remodeling, typically associated with PH, reduce the extent of blood perfusion throughout the lung [20] and, consequently, impairs ventilation–perfusion matching. Moreover, it is these adverse changes in blood flow distribution that are ultimately responsible for the increase in PAP [21]. This objective can best be achieved by visualizing blood flow distribution of the pulmonary circulation, in vivo, using microangiography.

We have previously demonstrated the validity and accuracy of synchrotron radiation (SR) microangiography for visualizing the distribution of pulmonary blood vessels (ID, >80 μm) in a closed-chest rat model with PH [20, 21]. Unlike conventional angiography methods, which have significant spatial and temporal resolution limitations, SR microangiography is effective for visualizing, not only the dense vascular branching network of the pulmonary microcirculation, but also the dynamic and regional changes in vessel caliber in response to specific vasoactive constrictors (e.g., ET-1) or dilators (e.g., NO).

In this study, we first aimed to assess the integrity of the pulmonary endothelium (i.e., endothelium-dependent vasodilation), and second, evaluate the contractile sensitivity of the vascular smooth muscle to exogenous ET-1 in normal, compared with pulmonary hypertensive rats. Importantly, we also aimed to assess the prophylactic potential of ghrelin for (1) preventing a reduction in blood flow distribution throughout the lung in PH, (2) maintaining normal endothelial function, and (3) preventing an enhanced ET-1-mediated vasoconstriction.

Materials and methods

Animals

All experiments were approved by the local Animal Ethics Committee of SPring-8, and conducted in accordance with the guidelines of the Physiological Society of Japan. Experiments were conducted on 17 male Sprague–Dawley rats (8 weeks old; B.W., ~180–220 g). Rats were divided into normoxic control rats (Cont-rats; n=7) and two groups of chronic hypoxic rats—saline-treated (CH-rats; n=5) and ghrelin-treated groups (CH+Ghr-rats; n=5). Two weeks prior to angiography experiments, the two groups of CH-rats were continuously housed in a hypoxic chamber (10± 0.1% O_2) for 2 weeks; except for a 10-min interval each day when the chamber was cleaned (Cont-rats remained in normoxic conditions). The hypoxic gas mixture was prepared from N_2 (gas cylinders) and compressed air and was continuously delivered to the hypoxic chamber at a flow rate of ~8 l/min. All rats were on a 12-h light/dark cycle at 25± 1°C and provided with food and water ad libitum.

Drug administration

All CH-rats that were to be placed into the hypoxia chamber, first received a subcutaneous injection of either saline (n=5) or ghrelin (150 μg/kg in 0.3 ml; n=5). CH-rats continued to receive daily injections of either saline or ghrelin during the 2 weeks of CH. Ghrelin was obtained from Peptide Institute Inc. and administered dissolved in saline as the vehicle.

Anesthesia and surgical preparation

On the day of experimentation, each rat was anesthetized with pentobarbital sodium (60 mg/kg, i.p.). Supplementary doses of anesthetic were periodically administered (~15 mg kg^{-1} h^{-1}, i.p.) to maintain a surgical level of anesthesia. Throughout the experimental protocol, body temperature was maintained at 37°C using a rectal thermistor coupled with a thermostatically controlled heating pad. The trachea was cannulated, and the lungs were ventilated with a rodent ventilator (SN-480-7, Shinano, Tokyo, Japan). A femoral artery and vein were cannulated for measurement of systemic arterial blood pressure (ABP) and drug administration, respectively. A 20-gauge BD Angiocath catheter (Becton Dickinson Inc., UT, USA), with the tip at a 30° angle, was inserted into the jugular vein and advanced into the right ventricle for administering contrast

agent as well as intermittently measuring right ventricular pressure (RVP).

SR microangiography

The pulmonary circulation of the anesthetized rat was visualized using SR microangiography at the BL28B2 beam line of the SPring-8 facility, Hyogo, Japan. We have previously described in detail the accuracy and validity of SR for visualizing the pulmonary microcirculation in the closed-chest rat [19]. The rat was securely fastened to a clear Perspex surgical plate, which was then fixed in a vertical position in front of the beam pathway, so that the SR beam would pass perpendicular to the sagittal plane from anterior to posterior through the rat thorax and ultimately to a SATICON X-ray camera.

Experimental protocol

Once the rat was positioned in the path of the X-ray beam, heart rate (HR) and ABP data were continuously recorded. RVP was also continuously recorded, except during vessel imaging, when the three-way stopcock on the right ventricle catheter was opened to a clinical autoinjector (Nemoto Kyorindo, Tokyo, Japan), which was used to inject a single bolus of contrast agent (Iomeron 350; Eisai Co. Ltd., Tokyo, Japan) at high speed (0.4 ml at 0.4 ml/s). For each 2-s period of scanning (a single exposure sequence), 100 frames were recorded. Rats were given at least 10 min to recover from each bolus injection of contrast agent.

Following baseline imaging, rats were exposed to acute hypoxia (8% O_2) for 5 min and then, upon recovery, administered in successive order (1) exogenous ET-1 (1 nmol/kg, i.v., Sigma, St. Louis, MO, USA), (2) the ET-1_A receptor antagonist, BQ-123 (1 mg/kg, i.v., Sigma, St. Louis, MO, USA), and (3) ACh (3.0 μg kg^{-1} min^{-1} for 5 min, i.v.) to assess endothelium-dependent vasodilation. Lung microangiography was performed after the fourth minute of hypoxia, the fifth minute following ET-1 and ACh injection/infusion, respectively, and 10 min after BQ-123 administration. The doses of all pharmacological agents used in this study are based on well-documented recommendations in the literature as well as our own preliminary experiments.

Morphometric analysis

Following the completion of each experiment, the rats were euthanized via anesthetic overdose and the heart excised. The atria were removed and the right ventricle wall separated from the left ventricle (LV) and septum. Tissues were blotted and weighed and normalized to 100 g body weight. Right and left ventricular weights were expressed as the ratio of the RV to the left ventricle + septum weight ($W_{RV}/W_{LV\ +\ septum}$, Fulton's ratio).

Cross sections of the left lung were fixed in 4% paraformaldahyde and subsequently embedded in paraffin. Sections 10-μm thick were stained with hematoxylin and eosin for examination by light microscopy. The wall-to-lumen ratio of the pulmonary arteries was measured in 34 muscular arteries (ranging in size from 150 to 400 μm in external diameter). To calculate the wall-to-lumen ratio, the internal diameter (ID) and outer diameter (OD) were measured using Image Pro-plus software (ver. 4.1, Media Cybernetics, MA, USA) and expressed as (OD − ID)/ID. Measurements were repeated along six different diameter planes transecting the center of each vessel and the average value recorded.

Immunohistochemistry

The following antibodies were purchased as indicated: Mouse monoclonal [TR.ET.48.5] to ET-1 (ab2786, Abcam). After fixation with 10% formalin (Sigma-Aldrich Ref. HT50-1-2) and embedding in paraffin, sections (5 μm thick) were deparaffinized and antigen retrieval was achieved using Mouse and Rabbit Specific HRP/DAB detection IHC kit (ab64264, Abcam). Immunostaining was evident by a brown precipitate at the antigen site. The sections were then lightly counter-stained with hematoxylin to visualize nuclei.

Data acquisition and analysis

The RVP and ABP signals were detected using separate Deltran pressure transducers (Utah Medical Products, Inc. UT, USA), the signals were relayed to Powerlab bridge amplifiers (ML117, AD Instruments Pty Ltd, Japan Inc.), and then continuously sampled at 500 Hz with an eight-channel MacLab/8s interface hardware system (AD Instruments), and recorded on a Macintosh Power Book G4 using Chart (v. 7.0, AD Instruments). HR was derived from the arterial systolic peaks.

All imaged vessel branches were counted. Vessels were categorized according to internal diameter (ID); 100–200 μm, 200–300 μm, and 300–500 μm. The ID of 57 vessels, comprising four branching generations, was measured in seven Cont-rats. The ID of 48 vessels was measured in five CH-rats. The ID of 72 vessels was measured in five CH+Ghr-rats. The ID of individual vessels was measured under basal conditions and then in response to each of the experimental conditions.

Image analysis

The computer-imaging program Image Pro-plus (ver. 4.1, Media Cybernetics, Maryland, USA) was used to enhance

contrast and the clarity of angiogram images (see Schwenke et al. [19] for a full description). The line-profile function of Image Pro-Plus was used as an accurate method for measuring the ID of individual vessels [20, 21]. A 50-μm thick tungsten filament, which had been placed directly across the corner of the detector's window, appeared in all recorded images, and was subsequently used as a reference for calculating vessel ID (in μm), assuming negligible magnification.

Statistical analysis

All statistical analyses were conducted using Statview (v5.01, SAS Institute, North Carolina, USA). All results are presented as mean±standard error of the mean (SEM). One-way ANOVA (factorial) was used to test for significant differences in (1) vessel caliber under basal conditions compared with each of the experimental conditions (e.g., ET-1, BQ-123) and (2) values for Cont-rats compared with either CH-rats or CH+Ghr-rats. Where statistical significance was reached, post hoc analyses were incorporated using the paired or unpaired *t* test with the Dunnet's correction for comparisons. A P value of ≤0.05 was predetermined as the level of significance for all statistical analysis.

Results

Baseline

Hemodynamic and morphometric analysis

Two weeks of CH induced pulmonary hypertension in saline-treated rats (Table 1), evident by a systolic RVP (sRVP) that was 70% above control values (P<0.01). CH also caused significant medial thickening of medium-sized pulmonary arteries (150 to 400 μm), which encompasses all vessel categories (Fig. 1a) resulting in an increase in the wall thickness-to-lumen diameter ratio (Fig. 1b). Collectively, the adverse increase in sRVP and medial thickening induced severe right ventricular hypertrophy in CH-rats (e.g., RV/LV+Sep ratio of 0.50, c.f. 0.30 in Cont-rats; Table 2). In comparison, the daily administration of ghrelin (150 μg kg^{-1} day^{-1}) during CH reduced the magnitude of PH (34% increase in sRVP; Table 1) and pulmonary vascular medial thickening (Fig. 1) such that the magnitude of right ventricular hypertrophy was also beneficially reduced (RV/LV+Sep ratio of 0.38; Table 2). Neither mean arterial blood pressure (MABP) nor HR were modified by CH in saline and ghrelin-treated rats.

Table 1 Cardiovascular variables of control rats (n=7) and chronic hypoxic rats (10% O_2 for 2 weeks) treated daily with subcutaneous injections of either "saline" (0.3 ml; n=5) or "ghrelin" (150 μg/kg in 0.3 ml saline; n=5)

	Control	Chronic hypoxia	
		Saline	Ghrelin
Body mass (g)	283±4	267±7	254±5††
sRVP (mmHg)	29.0±0.9	49.4±3.4††	39.1±1††*
MABP (mmHg)	123±7	121±12	106±5
HR (/min)	395±22	400±10	338±17*

Data are presented as mean ± S.E.M. † Significantly different from normoxia values (†P < 0.05; ††P <0.01). * Significant difference between 'Saline' and 'Ghrelin'. (*P < 0.05; **P < 0.01)

Synchrotron radiation microangiography

The increase in PAP in CH-rats was well correlated with a reduction in pulmonary blood flow distribution, which was assessed using SR microangiography. The baseline angiograms presented in Fig. 2a highlight the difference in the branching patterns for Cont-rats and CH-rats, ranging from the axial artery to the fourth generation of branching. The total number of vessel branches visible within each baseline image (i.e., 9.5×9.5 mm imaging window) was counted in the same region and field of view for each animal (Fig. 2b). CH significantly reduced the number of radiopaque vessels, primarily of the fourth branching generation, 25±1 for control rats compared

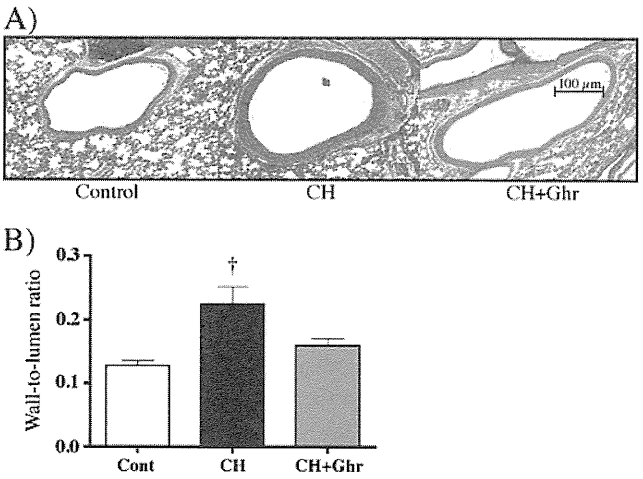

Fig. 1 **a** Histology photomicrographs of peripheral pulmonary arteries from control rats (*Cont*; n=7) and chronic hypoxic rats treated with either saline (*CH*; n=5) or ghrelin (*CH+Ghr*; 150 μg kg^{-1} day^{-1}; n=5). **b** Quantitative analysis of wall-to-lumen ratio in pulmonary arteries (ID=150–400 μm, which encompasses all vessel categories). Data are presented as mean±SEM. *P<0.05, significantly different from normoxia; †P<0.05, significant difference between chronic hypoxic rats treated with saline vs ghrelin

Table 2 Heart weight from three groups of rats: (1) control (n=7), (2) chronic hypoxia and saline for 2 weeks (n=5), and (3) chronic hypoxia and Ghrelin (n=5). Ghrelin (150 μg/kg; s.c.) was administered once a day

	Control	Chronic hypoxia	
		Saline	Ghrelin
Heart weight/ 100 g BW (mg)	284±10	345±10††	309±10†
RV/100 g (mg)	65±4	114±10††	84±3††*
LV + septum/ 100 g (mg)	219±9	230±2	225±3
RV/LV + septum	0.30±0.02	0.50±0.04††	0.38±0.02†*

Data are presented as mean ± S.E.M. † Significantly different from normoxia values ($^{\dagger}P < 0.01$; $^{\dagger\dagger}P < 0.001$). * Significant difference between 'Saline' and 'Ghrelin'. ($P < 0.05$)

with 17±1 branches for CH-rats, $P<0.05$ (Fig. 2b). In comparison, the concomitant administration of ghrelin during CH prevented the adverse reduction in vessel branching (22±1 of fourth generation branches), indicating that exogenous ghrelin acts to preserve pulmonary blood flow distribution during CH.

Immunohistochemistry of ET-1

Immunostaining was performed to "qualitatively" assess the expression of ET-1 protein in the endothelium of the left lung of control rats and CH-rats treated with saline or ghrelin. As illustrated in Fig. 3, positive staining (brown-red) was more apparent following 2 weeks of CH. However, ghrelin administration attenuated chronic hypoxia-induced over-production of ET-1 protein (i.e., no "excessive" intensity of positive staining), primarily within the pulmonary vessel endothelium (Fig. 3).

Responses to ET-1

In Cont-rats, exogenous ET-1 (1 nMol/kg, i.v.) caused mild pulmonary vasoconstriction, which was only significant for those vessels with an ID of 200–300 μm (Fig. 4) and, therefore, did not significantly increase sRVP (Fig. 5). Exposure to CH exacerbated the pulmonary vasoconstriction response to ET-1 for all vessel sizes tested (Fig. 2c), most notably in the 100–300-μm vessels, as quantified in Fig. 4. Consequently, ET-1 caused a large and significant 20±4% increase in sRVP ($P<0.01$). In comparison, the co-administration of ghrelin during CH prevented enhancement of ET-1 sensitivity, so that the magnitude of pulmonary vasoconstriction, and the consequential increase in sRVP, was similar to that of control rats (Figs. 4 and 5). ET-1 did not significantly change MABP or HR in Cont-rats and CH+Ghr-rats, but it did cause a significant 24% increase in MABP in CH-rats (Fig. 5).

Inhibition of Endothelin-1_A Receptor (BQ-123)

Administration of the ET-1_A receptor antagonist, BQ-123 (1 mg/kg), caused mild vasodilation of the pulmonary vessels, significant primarily for those vessels with an ID of 100–200 μm ($P<0.05$), similar for both control rats and CH+Ghr-rats (Fig. 4). In contrast, the vasodilatory response to BQ-123 in CH-rats was localized to only the mid-size vessels (ID=200–300 μm). Moreover, the sensitivity of these vessels to ET-1_A blockade was accentuated in the CH-rats, compared with control rats (Fig. 4). Consequently, the decrease in sRVP for CH-rats (11% decrease; $P<0.05$) was greater than that of control and ghrelin-treated rats (4% decrease; Fig. 5). BQ-123 did not significantly alter MABP or HR in all groups of rats (Fig. 5).

Endothelium-dependent vasodilation—responses to acetylcholine

ACh (3.0 μg kg^{-1} min^{-1} for 5 min, i.v.) caused pulmonary vasodilation in the pulmonary circulation of control rats, most notably in the 100–200-μm vessels (18% increase in ID), which was associated with a significant 12% decrease in sRVP (Figs. 4 and 5). In comparison, the pulmonary microvessels of untreated CH-rats were relatively non-responsive to ACh, displaying mild vasodilation only in the 100–200-μm vessels (NS, Fig. 4), which was not sufficient to cause a significant decrease in sRVP (Fig. 5). In those CH-rats treated with ghrelin, the vasodilatory response to ACh was still slightly blunted (11% increase in ID of the 100–200-μm vessels) although significantly less than that of the untreated CH-rats (Fig. 4). In both control rats and CH+Ghr-rats, ACh caused a decrease in MABP (significant only for control rats) without altering HR (Fig. 5).

Responses to acute hypoxia

Pulmonary vascular reactivity was assessed by exposing rats to acute hypoxia (8% O_2 for 5 min). The magnitude of acute hypoxic pulmonary vasoconstriction was not altered by CH, ghrelin, or a combination of both and, therefore, was similar for all groups of rats (Fig. 4c). In all rats, therefore, the magnitude of constriction tended to increase as vessel caliber decreased, with the greatest degree of vasoconstriction occurring in those vessels with a diameter between 100 and 300 μm. Similarly, the hemodynamic responses to acute hypoxia were similar for all groups of rats (Fig. 5). Therefore, acute hypoxia consistently induced a significant 21–23% increase in systolic RVP ($P<0.01$), a

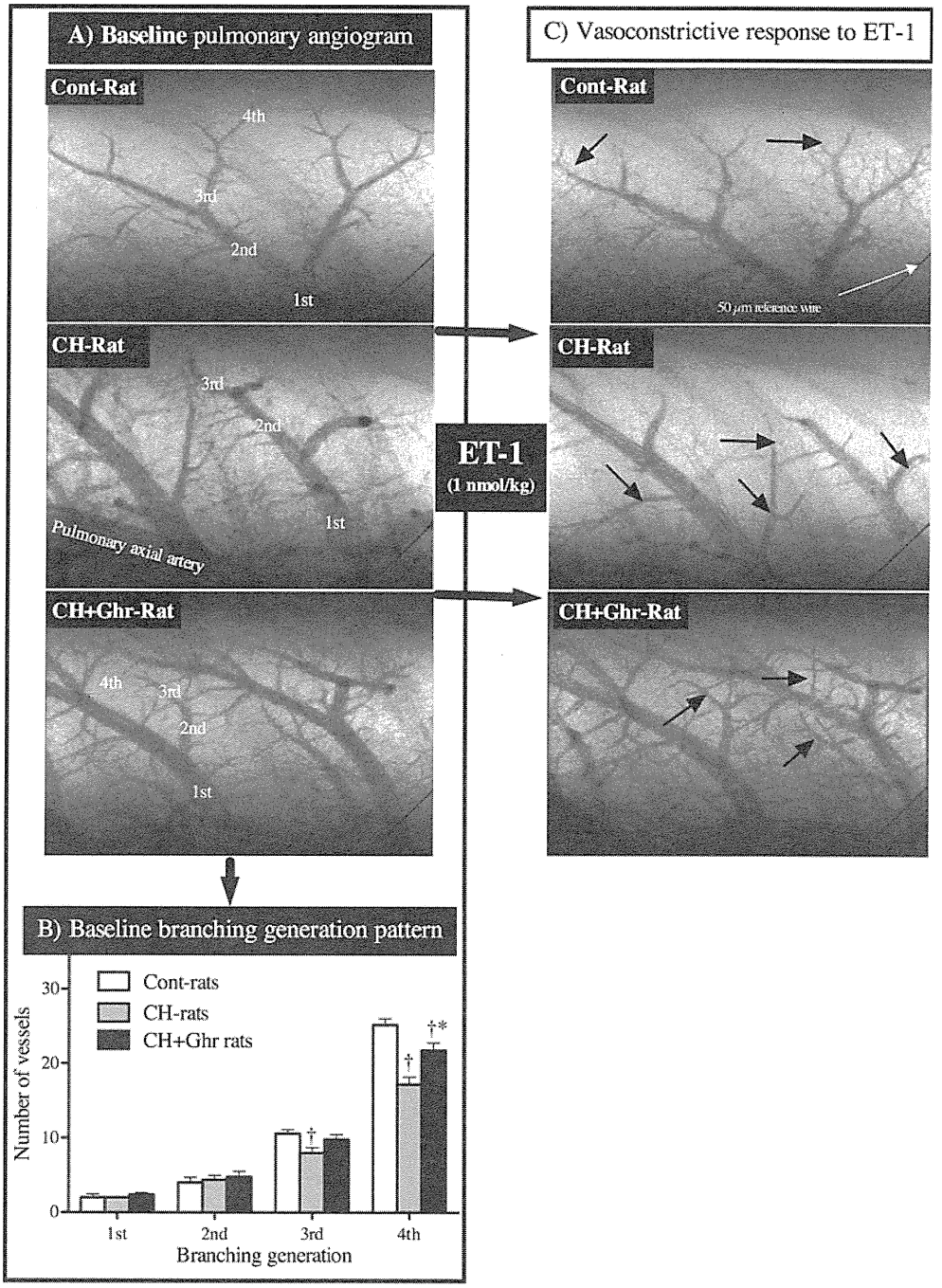

Fig. 2 *A* Microangiogram images showing the branching pattern of small pulmonary arteries in control rats (*Cont-rat*), chronic hypoxic rats (*CH-rat*), and CH-rats treated with ghrelin (*CH+Ghr-rat*). ***B*** The number of opaque vessels (mean±SEM) at each of the first four branching generations of the pulmonary circulation in Cont-rats (n=7), CH-rats (n=5), and CH+Ghr-rats (150 μg kg^{-1} day^{-1}; n=5). *C* Microangiograms illustrating vasoconstriction of pulmonary vessels (*black arrows*) in response to ET-1 (1 nmol/kg, i.v.) in control and CH+Ghr-rats but most notably in CH-rats. Pulmonary branches to the 4th generation from the left main axial artery were visible. The tungsten wire in the bottom right corner of each angiogram is a reference of 50-μm diameter. †P<0.05, significantly different from control rats; *P<0.05, significant difference between CH-rats and CH+Ghr-rats

decrease in MABP (39% to 59% decrease, P<0.01) but did not significantly change HR.

Discussion

The primary findings of this study demonstrate that the concomitant administration of ghrelin during CH attenuated the onset and development of PH by (1) reducing ET-1-mediated vasoconstriction, due to prevention of the over-production of ET-1 within the endothelium (qualitative only), (2) impeding pulmonary vascular remodeling and, ultimately, (3) preventing adverse changes in pulmonary blood flow distribution throughout the lung. These results suggest ghrelin may be a "prophylactic" treatment for those susceptible to developing PH, e.g., patients with a chronic obstructive pulmonary disorder.

The pulmonary vascular endothelium plays a critical role in modulating vascular tone with fine precision by releasing various vasoactive mediators, in particular ET-1 and NO, to ensure uncompromised perfusion of the lung for optimal ventilation/perfusion matching. Although the

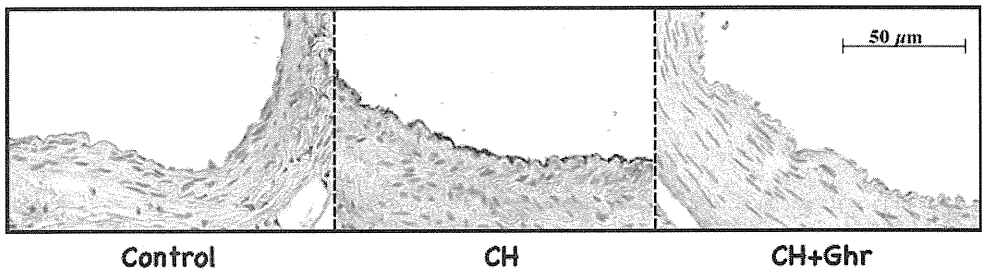

Fig. 3 Qualitative analysis of images from immunohistochemistry of ET-1 within the pulmonary vasculature of control rats (*Cont*) and chronic hypoxic rats treated with either saline (*CH*) or ghrelin (*CH+Ghr*; 150 μg kg^{-1} day^{-1})

pathomechanisms governing PH remain to be fully elucidated, it has become apparent that dysfunction of the pulmonary endothelium plays a critical role in the cascade of events that ultimately culminate in the development of PH [5, 18]. Importantly, endothelium-dependent release of NO is impaired [2, 10, 16] and the ET-1 vasoactive pathway is upregulated [4, 30]. This imbalance of the NO/ET-1 pathways significantly contributes to sustained vasoconstriction, endothelial and vascular smooth muscle cell proliferation, and an adverse increase in PAP [8, 24, 30].

Using the high-resolution benefits of SR microangiography, we showed in this study that untreated CH-rats had a blunted vasodilatory response to ACh, and an accentuated vasoconstriction response to exogenous ET-1, both indicative of endothelial dysfunction. Moreover, immunohistological analysis indicates that ET-1 protein levels within to the endothelium appear to be higher in untreated CH-rats, which concurs with our previous quantitative assessment of ET-1 mRNA in PH [23]. Using SR microangiography, we were also able to quantify the magnitude of dysfunction in this study and show that accentuation of the vasoreactivity responses to ET-1 (and BQ-123) was non-uniform so that the greatest vasoreactivity was located in the mid-sized arterioles (ID, ~200–300 μm) in PH. On the other hand, impairment of endothelium-mediated vasodilation (i.e., endothelial nitric oxide synthase (eNOS)), which also exhibits regional differences, is primarily localized to the small vessels (ID, ~100–200 μm) [22]. Thus, although eNOS and ET-1 are both non-uniformly distributed throughout the pulmonary circulation in PH, the pathological change appears to occur in different regions for eNOS (100–200-μm vessels) and ET-1 (200–300-μm vessels).

In accordance with our previous report [23], this study confirmed that exogenous ghrelin administration attenuated the development of PH in CH-rats. Interestingly, qualitative assessment (i.e., immunohistochemistry) suggests that

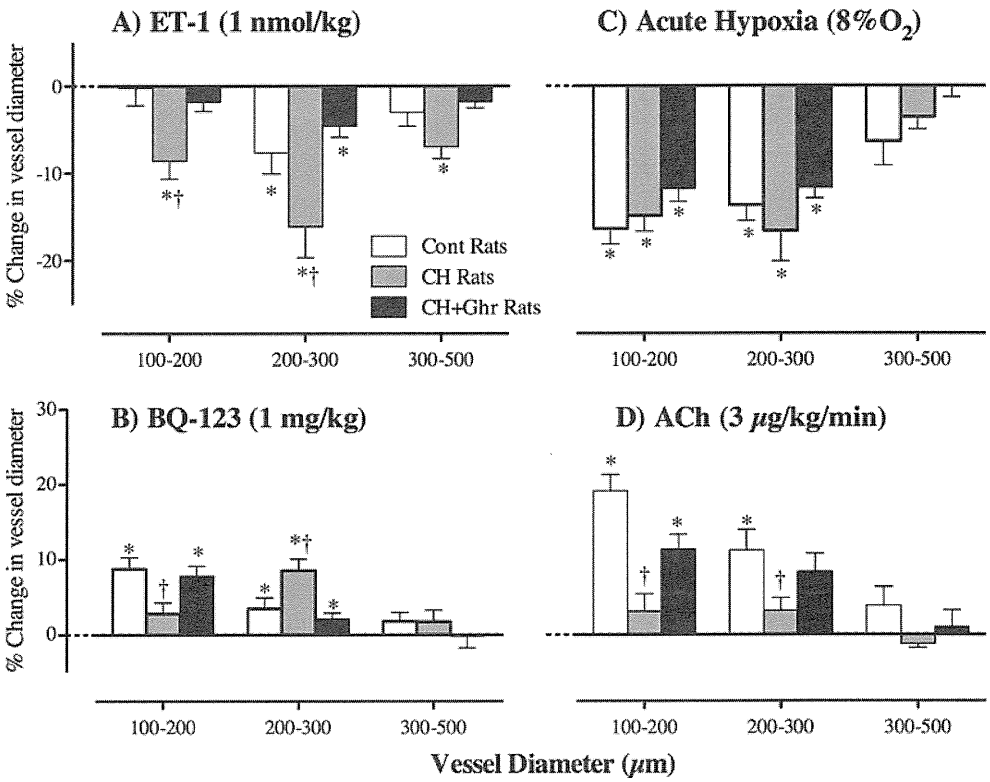

Fig. 4 The relationship between vessel size and the magnitude of pulmonary vasomotor responses (% change in vessel ID) in control rats (*Cont*) and chronic hypoxic rats treated with either saline (*CH*) or ghrelin (*CH+Ghr*) in response to the successive administration of **a** ET-1 (1 nmol/kg, i.v), **b** BQ-123 (1 mg/kg, i.v.), **c** acute hypoxia (8% O_2 for 5 min), and **d** ACh (3.0 μg kg^{-1} min^{-1} for 5 min). *$P<0.05$, significant reduction/increase in vessel caliber; †$P<0.05$, significant difference between Cont-rats and CH-rats

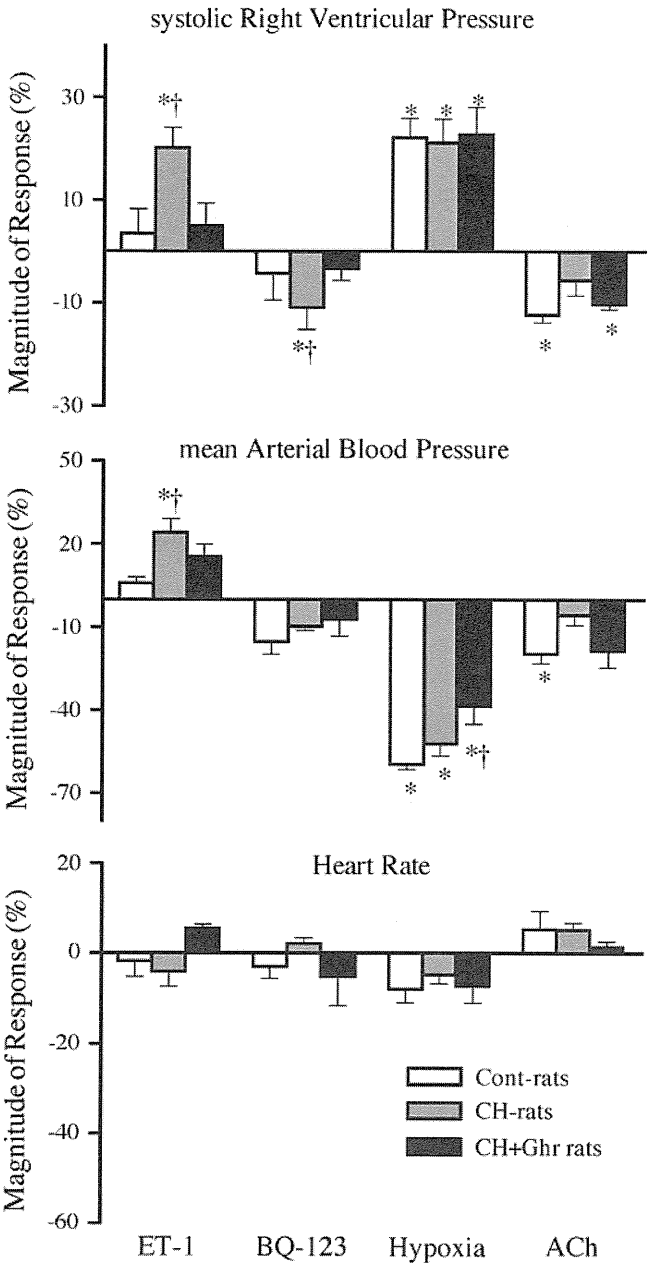

Fig. 5 Transient changes (% change) in sRVP, MABP, and HR in response to (1) ET-1 (1 nmol/kg, i.v), (2) BQ-123 (1 mg/kg, i.v.), (3) acute hypoxia (8% O_2 for 5 min), and (4) ACh (3.0 μg kg^{-1} min^{-1} for 5 min) for control rats (*Cont*) and chronic hypoxic rats treated with either saline (*CH*) or ghrelin (*CH+Ghr*). *$P<0.05$, significant increase/decrease in response to each intervention; †$P<0.05$, significantly different to Cont-rats

ghrelin-treated rats did not have an adverse increase in endothelial ET-1 protein synthesis. In this study, we also observed that the pulmonary vasoconstriction response to ET-1 was "normal" in ghrelin-treated CH-rats, and the endothelium-dependent vasodilation was less impaired, compared with untreated CH-rats. These results may suggest that ghrelin acts to maintain endothelium integrity—which could also help to prevent an over-expression of ET-1. The vasoactive effects of ET-1 and NO are reciprocally co-dependent such that, for example, the over-expression of ET-1 directly inhibits NO-mediated dilatation [3, 17]. Although this study highlights the benefit of ghrelin in preventing the adverse changes in the pulmonary vasculature, recent evidence by the Cardillo research team has shown that ghrelin is able to reverse, or normalize, an impaired balance between NO and ET-1 in the systemic circulation of patients with metabolic syndrome. Essentially, ghrelin improves the blunted endothelium-dependent vasodilation (increasing NO bioavailability) and reduces the vasoconstrictor effect of ET-1 [25–27].

Perhaps one of the most fundamental and novel findings of this study is that ghrelin was able to attenuate the adverse change in pulmonary blood flow distribution, assessed using SR microangiography that is normally associated with PH [20]. Indeed, vessel "rarefaction," typically evident in pulmonary angiograms of PH, was significantly attenuated in CH-rats treated with ghrelin (see Fig. 2). It seems reasonable to propose that this preservation of pulmonary blood flow distribution is likely a culmination of (1) ghrelin's direct vasodilatory effects (via GHS receptors), (2) ghrelin's ability to maintain an intact endothelium, (3) ghrelin's down-regulation of ET-1 synthesis [9, 28, 29] (and increase in NO bioavailability), and (4) attenuation of vascular remodeling.

In this study, we demonstrated that chronic ghrelin treatment prevented adverse changes in the ET-1 vasoactive pathway and, importantly, pulmonary blood flow distribution. However, one limitation of this study is that we did not determine whether an acute bolus of ghrelin was able to improve pulmonary hemodynamic function in CH-rats that already had well-established PH. Such experiments are critical to fully establish the effectiveness of ghrelin for clinically treating, not only preventing, PH. Interestingly, Tesauro et al. [27] reported that ghrelin "acutely" restored normal systemic endothelial function in metabolic syndrome patients with existing endothelial dysfunction, evident by "normal" NO-dependent vasodilation and ET-1 vasoconstriction.

Acute hypoxic pulmonary vasoconstriction

Acute hypoxic pulmonary vasoconstriction (HPV) is an important intrinsic homeostatic mechanism of the pulmonary circulation for regulating the regional distribution of blood flow and, thus, optimizing gas exchange within the normal lung. In this study, we observed that the acute HPV was not altered by chronic hypoxia (i.e., PH), which is consistent with our previous studies [20, 21]. More importantly, however, we reported that the HPV was not altered in ghrelin-treated rats. These results indicate that the prophylactic use of ghrelin in PH does not adversely alter the HPV—which is an essential requirement to ensure